Journal of proteome research

pubs.acs.org/jpr

Article

Proteomic Serum Profiling of Holstein Friesian Cows with Different Pathological Forms of Bovine Paratuberculosis Reveals Changes in the Acute-Phase Response and Lipid Metabolism

Alejandra Isabel Navarro León,[#] Marta Muñoz,[#] Natalia Iglesias, Cristina Blanco-Vázquez, Ana Balseiro, Fátima Milhano Santos, Sergio Ciordia, Fernando J. Corrales, Tania Iglesias, and Rosa Casais*

Cite This: *J. Proteome Res.* 2024, 23, 2762−2779

Read Online

ACCESS | Metrics & More | Article Recommendations | Supporting Information

ABSTRACT: The lack of sensitive diagnostic methods to detect *Mycobacterium avium* subsp. *paratuberculosis* (Map) subclinical infections has hindered the control of paratuberculosis (PTB). The serum proteomic profiles of naturally infected cows presenting focal and diffuse pathological forms of PTB and negative controls (n = 4 per group) were analyzed using TMT-6plex quantitative proteomics. Focal and diffuse are the most frequent pathological forms in subclinical and clinical stages of PTB, respectively. One (focal versus (vs.) control), eight (diffuse vs. control), and four (focal vs. diffuse) differentially abundant (DA) proteins (q-value < 0.05) were identified. Ingenuity pathway analysis of the DA proteins revealed changes in the acute-phase response and lipid metabolism. Six candidate biomarkers were selected for further validation by specific ELISA using serum from animals with focal, multifocal, and diffuse PTB-associated lesions (n = 108) and controls (n = 56). Overall, the trends of the serum expression levels of the selected proteins were consistent with the proteomic results. Alpha-1-acid glycoprotein (ORM1)-based ELISA, insulin-like growth factor-binding protein 2 (IGFBP2)-based ELISA, and the anti-Map ELISA had the best diagnostic performance for detection of animals with focal, multifocal, and diffuse lesions, respectively. Our findings identify potential biomarkers that improve diagnostic sensitivity of PTB and help to elucidate the mechanisms involved in PTB pathogenesis.

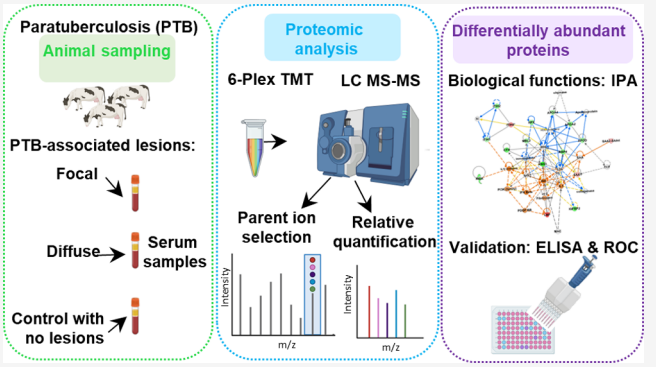

KEYWORDS: *paratuberculosis, Mycobacterium avium subsp. paratuberculosis, cattle, serum proteome, biomarkers, diagnosis, acute-phase proteins, pathogenesis, disease progression*

1. INTRODUCTION

Paratuberculosis (PTB) or Johne's disease is a widespread chronic enteritis caused by *Mycobacterium avium* subspecies *paratuberculosis* (Map) that affects domestic and wild ruminants. It has a heavy economic impact on the dairy industry worldwide due to reduced milk production, premature culling, reduced slaughter value, and continued spread of infection.[1,2] PTB has also been related to reduced fertility rates[3,4] and increased susceptibility to other diseases, particularly mammary infections.[5] The relevance of this disease would be even greater when considering its zoonotic potential and the risk of transmission of viable Map through pasteurized milk and milk products.[6−8] The association of Map with human autoimmune diseases like Crohn's disease, type I diabetes, multiple sclerosis, and rheumatoid arthritis has been documented.[9−15]

Map transmission primarily occurs by the fecal-oral route through the ingestion of Map contaminated feces, colostrum, or milk. Infection usually occurs within the first months of life of the animal but remains subclinical for an average of 2−5 years before becoming clinical in a small percentage of cases. Paratuberculosis clinical symptoms are chronic enteritis (with persistent diarrhea), severe weight loss (cachexia), and low milk yield.[16] Map can enter a herd through purchase of subclinically infected cattle and contaminated feces adhering to vehicles, equipment, and visitors. Once in the herd, the spread of Map is mainly due to its extremely long subclinical period during which the host is intermittently shedding Map in feces, contaminating the environment, and transmitting the pathogen to progeny and other members of the herd.[17] In this context, early detection of subclinical animals is critical for more effective disease control within the herds. Currently, most control programs are based on

Special Issue: Women in Proteomics and Metabolomics

Received: April 24, 2023
Revised: September 18, 2023
Accepted: September 22, 2023
Published: October 20, 2023

Table 1. Infectious Status of the Animals (n = 12) Used for the Proteomic Analysis of Sera from Holstein Friesian Cows with Different Pathological Forms of Bovine Paratuberculosis and Control Animals with No Lesions Detected[a]

ID	histological group	infectious status	clinical signs	ZN	Anti-Map ELISA	PCR feces	PCR tissues	culture feces	culture tissues	age (years)
1	without lesions	Not infected	NO	NEG	NEG (1.26)	NEG	NEG	NEG	NEG	2.70
2	without lesions	Not infected	NO	NEG	NEG (2.45)	NEG	NEG	NEG	NEG	1.27
3	without lesions	Not infected	UN	NEG	NEG (5.44)	NEG	NEG	NEG	NEG	3.26
4	without lesions	Not infected	UN	NEG	NEG (8.84)	NEG	NEG	NEG	NEG	0.81
5	focal	Infected	NO	POS (+)	SUS (47.25)	INC	NEG	NEG	NEG	4.10
6	focal	Infected	NO	POS (+)	NEG (2.64)	NEG	POS	NEG	POS	4.71
7	focal	Infected	NO	POS (+)	NEG (1.09)	NEG	NEG	NEG	POS	4.39
8	focal	Infected	NO	POS (+)	NEG (2.37)	NEG	NEG	NEG	POS	2.12
9	diffuse intermediate	Infected	YES	POS (++)	POS (205.94)	POS	POS	NEG	POS	5.22
10	diffuse intermediate	Infected	YES	POS (++)	POS (254.72)	POS	POS	POS	POS	6.01
11	diffuse intermediate	Infected	YES	POS (++)	POS 113.49)	POS	POS	NEG	NEG	5.09
12	diffuse multibacillary	Infected	YES	POS (+++)	POS (157.83)	POS	POS	NEG	POS	4.82

[a]ID, cows' identification; UN, undetermined; SUS, samples with the sample/positive control ratio greater than 45% and lower than 55% are considered suspect; the number of + shown in parentheses in the Ziehl-Neelsen (ZN) column refers to the amount of acid-alcohol resistant bacteria present; in the anti-Map ELISA column, the numerical value obtained in the ELISA is shown in parentheses; INC, inconclusive result after repeating the analyses twice.

the "test and cull" policy combined with the establishment of good management practices.[18] Several diagnostic techniques are used to detect Map-infected cattle; however, their performance has limitations and varies widely depending on the stage of Map infection.[19−21] Conventional diagnostic methods have low sensitivities for detection of subclinical infection as the bacteria are excreted in low numbers, and animals have low titers of anti-Map antibodies. Thus, fecal culture sensitivity is 70% for cattle with clinical signs associated with PTB and 23−29% for cattle with no detectable clinical signs.[22] PCR sensitivity and specificity were estimated to be 29% and 99.3%, respectively.[23] The antibody response to Map infection is only detectable by ELISA late in infection.[21] The sensitivity of ELISAs, used to detect anti-Map antibodies, also varies depending on the stage of infection (50−87% in cattle with clinical signs, 24−94% in cattle with no clinical signs but shedding Map, and 7−22% in infected cattle with no clinical signs and no shedding).[22] ELISAs specificity varies between 40 and 100% depending on several factors such as the test used, exposure to other environmental bacteria, Map vaccination, and previous intradermal tuberculosis test.[22]

Consequently, the identification of one or more easily measured biomarkers with high diagnostic performance would be very important for PTB global control.

Host biomarkers have been postulated as tools to develop novel diagnostic methods for PTB.[24−37] Some have been validated for detection of naturally infected cattle in various stages of Map infection.[38−42] Several proteomic studies to investigate the host proteome response to mycobacterial infections and specifically to Map infection have been performed to identify biomarkers of Map infection for development of new diagnostic tools. These studies might also help to identify potential candidate genes for selective breeding programs to enhance resistance or tolerance to PTB.[43] Identification of biomarkers in plasma or serum is an effective method for disease diagnosis since blood samples are easy to collect and proteins are the ultimate players in biological activities. So, changes in the proteomic profiles of infected animals will also help to understand PTB pathogenesis and disease progression. The variations in the circulating peptidomes of animals experimentally infected with either *Mycobacterium bovis*, the causative etiological agent of tuberculosis (TB), or Map at different times postinfection using high-resolution proteomics approaches (iTRAQ) was studied by Seth et al. (2009).[24] These authors found that vitamin D binding-protein precursor (GC), alpha-1 acid glycoprotein (ORM1), alpha-1B glycoprotein, fetuin B (FETUB), and serine proteinase inhibitor were identified in both infections. Transthyretin (TTR), retinol binding proteins (RBPs), and cathelicidin (CATHL) were exclusively identified in Map infection, while alpha-1 microglobulin/bikunin precursor protein, ORM1, FETUB, and alpha-1B glycoprotein were elevated exclusively in *M. bovis* infected animals. Proteomic analysis by 2-dimensional fluorescence difference gel electrophoresis (2D-DIGE) of plasma from Holstein cows testing strongly positive or negative to anti-Map antibodies by ELISA was carried out by You et al. (2012).[25] They identified other potential biomarkers, different from the ones previously mentioned, six up-regulated proteins (p-value < 0.05) (transferrin (TF), gelsolin (GSN) isoforms alpha and β, complement subcomponent C1r (C1R), complement component C3 (C3), amine oxidase copper containing 3 (AOC3), and coagulation factor II (F2)) and two down-regulated (coagulation factor XIII-B polypeptide (COAFXIII) and fibrinogen γ chain (FGG) and its precursor) in ELISA positive animals with respect to the negative controls.

Biomarker discovery has also been performed for other mycobacteria, host species, and sample types. The circulating *M. bovis* peptides and host response proteins as biomarkers for unambiguous detection of subclinical infection have been investigated.[44] Between the identified host biomarkers, GC showed the greatest sensitivity and specificity for the detection of *M. bovis*. Label-free quantitative proteomics was used to identify novel plasma biomarkers for discriminating pulmonary TB and latent infection.[45] These authors studied the molecular mechanism behind the progression from latent to active TB and identified plasma individual biomarkers for discriminating both types of TB. They proposed an ideal diagnostic model consisting of alpha-1-antichymotrypsin, ORM1, and E-cadherin with high sensitivities and specificities to discriminate latent from active TB and active from healthy controls.

Proteomic profiling of serum from Map-infected sheep at different times postinfection identified two putative serum

https://doi.org/10.1021/acs.jproteome.3c00244
J. Proteome Res. 2024, 23, 2762−2779

Table 2. Infectious Status and Age of the Animals Used for Validation by ELISA of the Differentially Abundant Proteins Selected after Proteomic and Functional Analysis[a]

	control group (n = 56)	focal group (n = 61)	multifocal group (n = 25)	diffuse group (n = 22)
Clinical signs	0%	6.56%	24.0%	63.64%
Ziehl-Neelsen	UN	65.57%	96.0%	100%
Anti-Map antibodies serum ELISA	0%	4.91%	16.0%	77.27%
Fecal real time PCR	0%	11.48%	32.0%	72.73%
Fecal bacteriological culture	0%	4.91%	8.0%	27.27%
Tissue real time PCR	UN	27.87%	48.0%	77.27%
Tissue bacteriological culture	UN	21.31%	28.0%	63.63%
Mean age (years)	3.90 ± 2.35	5.59 ± 2.24***	5.24 ± 1.80	5.47 ± 1.91*

[a]UN, undetermined because no tissues were available from these animals; asterisks indicate whether differences between each histopathological group and the control are or are not significant (* $p < 0.05$, *** $p < 0.001$).

biomarkers (TTR and alpha hemoglobin).[46] They are acute-phase proteins (APPs) present in the serum proteome that have also been identified as serum biomarkers in human inflammatory conditions and cancer. Other studies[47] have investigated the macrophage proteome at different stages of Map infection revealing a mechanism of pathogen dissemination. The proteome changes that Map induces after incubation in milk at 37 °C (mammary gland) and 4 °C (tank milk) in comparison to Map from M7H9 broth at 37 °C have also been studied.[48]

The aim of the present study was to obtain the serum proteomic profiles of Holstein Friesian cows with different histopathological forms of PTB (focal and diffuse) and control animals without PTB-associated histological lesions detected. TMT-6plex quantitative proteomics was used to identify differentially abundant (DA) proteins between groups (focal versus (vs.) control, focal vs diffuse, and diffuse vs control) and host pathways activated during infection to reach a better understanding of the pathogenesis of the disease and to provide new potential biomarkers for Map infection. The diagnostic potential of six of the DA proteins was further evaluated by specific ELISA using serum samples from 61 animals with focal, 25 with multifocal, 22 with diffuse histological lesions, and 56 PTB-free animals.

2. MATERIALS AND METHODS

2.1. Animals and Samples

Sera collected from three groups of animals: (1) naturally infected Holstein Friesian cows with focal pathological forms of bovine PTB (n = 4); (2) naturally infected Holstein Friesian cows with diffuse pathological forms of bovine PTB (n = 4); and (3) negative control animals with no PTB-associated lesions detected (n = 4) were analyzed using TMT-6plex quantitative proteomics. The infectious status of these 12 animals was determined by histopathology, specific antibody anti-Map serum ELISA test (anti-Map ELISA), bacteriological culture, and specific real-time polymerase chain reaction (PCR) of tissues and feces following the procedures previously described[40] (Table 1). Histopathology was used as the gold standard for this study. Animals were classified as focal, multifocal, diffuse, and without lesions detected.[49] The average age of the control, focal, and diffuse groups was 2.01 ± 1.16, 3.83 ± 1.17, and 5.28 ± 0.51, respectively, ranging from 0.81 to 6.01 years old. Significant differences in the mean age between groups were found for the comparison of diffuse vs. control (p = 0.003). Animals with focal histological lesions were chosen so none of them showed PTB-associated clinical signs and were positive at least by one of the diagnostic techniques used to confirm that these animals were infected. Focal animals were 100% positive by Ziehl-Neelsen (ZN), a histological technique to specifically visualize acid-fast bacilli (AFB), 25% positive by anti-Map ELISA and tissue real-time PCR, and 75% positive by tissue bacteriological culture isolation. Diffuse animals, representing a more advance stage of the disease, were chosen so 100% of the animals showed clinical signs and were positive by ZN, anti-Map ELISA, and fecal and tissue real-time PCR. Moreover, 75% were positive by intestinal tissue culture and 25% by fecal bacteriological culture. Animals included in the control group were negative by all the diagnostic techniques used. The members within each established group share the same type of histological lesion; however, the age and specific infectious status (Table 1) of each animal within a group are different, and there is a high intraheterogeneity within each group. After proteomic analysis, selected DA proteins were validated using a set of serum samples from 108 infected animals with focal (n = 61), multifocal (n = 25) and diffuse lesions (n = 22, 1 diffuse paucibacillary, 14 diffuse intermediate, and 7 diffuse multibacillary) and 56 control animals from PTB-free farms. The infectious status of these animals is summarized in Table 2 (see also Supplementary Table 1 for the complete results data set).

As we can see in Table 2, the percentage of positivity increases as does the severity of the histological lesions. The PTB-free status of the negative reference animals from farms with no prior history of clinical disease was verified yearly by repeatedly negative anti-Map serum ELISA results during 3 consecutive years depending on the specific farm and was also confirmed by fecal real-time PCR and bacteriological isolation once at culling. Significant differences in the mean age of the animals were detected between the focal and diffuse groups vs. the PTB-free control ($p < 0.001$ and $p = 0.027$, respectively); however, no significant differences were observed for the multifocal vs. PTB-free control, multifocal vs. focal, multifocal vs. diffuse, and focal vs. diffuse comparisons.

Samples of blood and feces were collected from all the animals included in the study. Tissue samples (ileocecal valve, distal jejunum, and distal jejunal and ileal lymph nodes) were taken from animals with focal, multifocal, and diffuse histological lesions *in situ* after evisceration in the abattoirs and split for molecular, microbiological, and histopathological analysis. No tissues were available for histological analysis from the PTB-free animals used in the validation. Blood samples were drawn from the tail vein into Vacuette tubes Z serum clot activator of 4.5 mL (Greener BIO-ONE, Kremsmünster, Austria) and then transported to the laboratory, and serum samples were separated by centrifugation at 1000g (2500 rpm) for 20 min at room temperature and then stored at −80 °C for subsequent analysis.

https://doi.org/10.1021/acs.jproteome.3c00244
J. Proteome Res. 2024, 23, 2762−2779

2.2. Ethical Statement

Experimental procedures were approved by the SERIDA Animal Ethics Committee and authorized by the Regional Consejería de Agroganadería y Recursos Autóctonos del Principado de Asturias − Spain (authorization codes PROAE 29/2015 and PROAE 66/2019). All the procedures were carried out following Directive 2012/63/EU of the European Parliament and the Spanish RD53/2013. Peripheral blood and fecal samples were collected by trained personnel and in accordance with good veterinary practice.

2.3. Serum Proteomic Analysis

Sera from 12 naturally infected Holstein Friesian cows with different pathological forms of PTB (focal and diffuse) and negative control animals with no lesions detected (four biological replicates per group) were collected and analyzed using TMT-6plex quantitative proteomics to identify DA proteins between groups.

FPLC Seppro IgY-14 LC10 columns (Sigma, St. Lous, MO) were used to deplete the 14 high-abundance proteins in serum (albumin, IgG, apolipoproteins, etc.) to enrich the low abundance protein fraction enhancing the resolution of low expressed proteins. The depletion was performed from 100 μL of each serum sample diluted with TBS (10 mM Tris-HCl, 150 mM NaCl) according to the manufacturer's instructions. The protein concentration in each sample was quantified by the Pierce method at 660 nm and 200 μg precipitated with methanol/H_2O/chloroform (4/3/1, %v/v). The protein pellet was resuspended in 32 μL of digestion buffer (7 M urea, 2 M thiourea, and 100 mM TEAB), and the amount of protein was quantified again by the same method. After the reduction of disulfide bridges with 5 mM tris (2-carboxyethyl) phosphine hydrochloride (TCEP) and subsequent alkylation with 10 mM chloroacetamide (CAA), 40 μg of each sample was digested with trypsin (1:20 enzyme:protein ratio). After overnight digestion at 37 °C, samples were dried down in a SpeedVac, and TMT 6-plex isobaric labeling was performed following the manufacturer's protocols. Upon labeling, individual samples were combined according to the following scheme: TMT-6plex pool I included samples from cows 1, 2, 5, 6, 9, and 10, and TMT-6plex pool II included samples from cows 3, 4, 7, 8, 11, and 12 (see Table 1). Each TMT pool was lyophilized using the SpeedVac concentrator and quantified by fluorimetry (Qubit). Peptides for each experiment were then separated using the Pierce High pH Reversed-Phase Peptide Fractionation kit, according to the manufacturer's instructions, and cleaned using the Reversed-Phase C18 Stage-Tips. Then, 1 μg of each fraction was solubilized using solvent A (2% acetonitrile [ACN] in water, 0.1% FA) and subjected to liquid chromatography coupled to Triple-TOF mass spectrometry (nano LC-ESI-MSMS) analysis using a nano liquid chromatography system (Eksigent Technologies nanoLC Ultra 1D plus, SCIEX, Foster City, CA, USA) coupled to a Triple-TOF 5600 mass spectrometer (SCIEX, Foster City, CA, USA) via a Nanospray III source. Chromatographic separation was performed on a C18 Acclaim PepMap 100 analytical column (Thermo Scientific, 75 μm × 15 cm, 1.7 μm, 130 Å). Peptides were fractionated at a flow rate of 250 nL/min in a 250 min gradient with increasing concentrations of ACN (2% to 90%). A Triple-TOF 5600 system was operated in positive ion mode as follows: ion spray voltage 2300 V, curtain gas (CUR) 35, interface heater temperature (IHT) 150 °C, ion source gas 1 (GS1) of 25, and declustering potential (DP) of 100 V. Data were acquired in information-dependent acquisition (IDA) mode with AnalystTF 1.7 Software (SCIEX, USA). IDA parameters were as follows: survey scan in the mass range of 350−1250 m/z, accumulation time 250 ms, followed by MS2 spectrum accumulation for 150 ms (100−1800 m/z) in a cycle of approximately 4 s. MS/MS fragmentation was performed in the 100−1250 m/z range considering a charge state of 2−5. Dynamic exclusion was set to 15 s. IDA rolling collision energy (CE) parameter script was used to control the CE. The MS/MS spectra were acquired in high sensitivity mode with 'adjust collision energy when using iTRAQ reagent' settings. The mass spectrometry data obtained were processed using PeakView 2.2 software (SCIEX, Foster City, CA, USA) and exported as mgf files. Proteomics data analysis was performed by using 4 search engines (Mascot Server v2.5.1, OMSSA, X!Tandem, and Myrimatch) against the *Bos taurus* protein database (UniProt knowledgebase) in order to identify labeled peptides and determine relative abundance at a >95% confidence interval. A false discovery rate (FDR) estimation procedure was applied for peptide identification, and only peptides passing FDR < 1% cutoff were considered reliable hits.[50] Differential regulation was measured using linear models, as previously described,[51] and statistical significance was measured considering q-values < 0.05. DA proteins were classified into four categories: confident (q-value < 0.01), likely (q-value < 0.05), putative (q-value >0.05 but p-value <1-π0), and not differentially regulated (q-value > 0.05 and p-value > 1-π0). The proteomics data were deposited in the Pride database (PXD04162). The reproducibility of the samples across the two TMT-6plex experiments (pool I and pool II) was assessed, and no bias was detected between them. For both, focal vs control and diffuse vs control contrasts, most log2 fold change measurements were highly reproducible across sample sets (see Supplementary Figure 1).

Network analysis was carried out using the Ingenuity Pathway Analysis (IPA) software tool including the list of all the DA proteins (n = 19 for focal vs. control from which IPA recognized 16; n = 49 for focal vs. diffuse, 37 recognized by IPA; and 113 diffuse vs. control, 69 recognized) in the categories confident, likely, and putative. Considering the high heterogeneity of the samples within each histopathological group, putative DA proteins were also considered for functional analysis, and proteins of interest were further validated using other techniques to confirm their expression changes. Canonical signaling pathways enriched by the DA proteins were identified and classified according to p-values. The Z-scores linked to canonical signaling pathways were also determined. Z-scores were represented by orange or blue colors and indicated the activation ($Z > 0$) or inhibition ($Z < 0$) of the canonical signaling pathway, respectively. IPA core analysis identified the top diseases and disorders, canonical pathways, and functional networks significantly related to the changes observed in the proteome of the infected animals.

Representative networks obtained by IPA analysis are depicted with upregulated proteins shown in red and down-regulated proteins in green (light red and green indicate less extreme increased or decreased measurement in the data set). Orange indicates the prediction of activation of a pathway and blue prediction of inhibition (lighter orange and blue indicate that the prediction has been done with less confidence). Solid lines indicate direct connections, while dotted lines indicate indirect connections (circular arrows mean influence itself). The pointed and blunt arrowheads represent activating and inhibitory relationships, respectively. Orange line indicates

https://doi.org/10.1021/acs.jproteome.3c00244
J. Proteome Res. 2024, 23, 2762−2779

Table 3. Differentially Abundant Proteins (q-value < 0.05) Identified by TMT-6plex Quantitative Proteomics Analysis of Serum of Holstein Friesian Cows with Different Pathological Forms of Paratuberculosis and Control Animals with No Detected Lesions[a]

comparison	category	Log2_fold_change	q-value	p-value	inferred proteins	description	location
Foc vs Ctrl	**confident.up**	**1.576**	**0.003**	**0.000007**	**Q3SZR3**	**Alpha-1-acid glycoprotein (ORM1)**	**SEC**
Dif vs Ctrl	confident.down	−4.649	0.000	0.000001	A0A0A0MPA0	Serpin domain-containing protein (LOC784932)	SEC
Dif vs Ctrl	confident.up	1.759	0.000	0.000001	Q58D62	Bovine Fetuin-B (FETUB)	SEC
Dif vs Ctrl	**confident.up**	**1.361**	**0.003**	**0.000029**	**Q3SZR3**	**Alpha-1-acid glycoprotein (ORM1)**	**SEC**
Dif vs Ctrl	**likely.up**	**2.692**	**0.015**	**0.000190**	**P13384**	**Insulin-like growth factor-binding**protein 2 (IGFBP2)	**SEC**
Dif vs Ctrl	likely.up	4.441	0.026	0.000417	Q3MHN5	Vitamin D-binding protein (GC)	SEC
Dif vs Ctrl	likely.down	−1.333	0.032	0.000625	P35541	Serum amyloid A protein (SAA)	SEC
Dif vs Ctrl	likely.up	1.628	0.044	0.001000	Q29RU4	Complement component C6 (C6)	SEC
Dif vs Ctrl	likely.up	3.760	0.048	0.001250	A0A3Q1M820	Sacsin molecular chaperone (SACS)	CM
Foc vs Dif	**confident.up**	**1.670**	**0.005**	**0.000014**	**Q2TBI0**	**Lipopolysaccharide-binding protein (LBP)**	**SEC**
Foc vs Dif	confident.down	−1.816	0.003	0.000015	P00921	Carbonic anhydrase 2 (CA2)	CM, CYT
Foc vs Dif	confident.up	1.945	0.003	0.000023	A0A0A0MPA0	Serpin domain-containing protein (LOC784932)	EXS
Foc vs Dif	likely.down	−1.549	0.028	0.000312	P01045	Kininogen-2 (KNG2)	SEC, EXS

[a]Three comparisons were performed: Foc/Ctrl, focal versus (vs) control; Dif/Ctrl, diffuse vs. control; and Foc/Dif, focal vs. diffuse. Proteins listed were ordered by q-value. SEC, secreted; EXS, extracellular space; CYT, cytoplasm; CM, cell membrane; differentially abundant (DA) proteins were classified into two categories according to the following criteria (confident if q-value <0.01 and likely if q-value <0.05). In the inferred proteins column, we indicate the protein accession numbers. In bold face are shown 3 DA proteins that were selected to be further validated by ELISA.

activation, blue inhibition, yellow indicates that findings are inconsistent with the state of downstream molecule, and gray effect indicates no predicted effect.

2.4. Enzyme-Linked Immunosorbent Assay (ELISA) Analysis of Differentially Abundant Proteins

For further validation of DA-selected proteins bovine IGFBP2, ORM1, complement factor H (CFH), bovine antithrombin III (SERPINC1), kininogen 1 (KNG1), and lipopolysaccharide (LPS)-binding protein (LBP), their serum concentration was measured for each animal using commercially available ELISA kits according to the manufacturer's instructions (MyBioSource, San Diego, CA, USA). Briefly, IGFBP2 ELISA is a sandwich ELISA for *in vitro* quantitative measurement of bovine IGFBP2 in serum, plasma, tissue homogenates, and other biological fluids. The plate is precoated with an antibody specific to bovine IGFBP2 and after adding the samples they are incubated with a biotin-conjugated antibody specific to IGFBP2. The analytical sensitivity, defined as the minimum detectable dose, is less than 0.32 ng/mL, the detection range is 0.94−60 ng/mL, and no significant cross-reactivity or interference between IGFBP2 and analogues form other species is observed. The intra-assay coefficient of variation (CV) is <10% and interassay <12%; ORM1 ELISA is based on a competitive ELISA technique that utilizes a polyclonal antibovine ORM1 antibody and antibovine ORM1-HRP conjugate for detection of bovine ORM1 in cell culture supernatants, body fluids, and tissue homogenate. ORM1 ELISA has an intrabatch CV and interbatch <10%, analytical sensitivity 1 ng/mL, detection range 1−250 ng/mL and no significant cross-reactivity between ORM1 and other analogues observed; CFH competitive ELISA is like the ORM1 ELISA but using specific polyclonal antibovine CFH antibody and antibovine CFH-HRP conjugate. CV intra and interbatch str <10%, analytical sensitivity is 1 ng/mL, detection range 1−500 ng/mL, and no significant cross-reactivity between CFH and other analogues is observed; bovine SERPINC1 ELISA kit is a quantitative sandwich ELISA with a analytical sensitivity of 2.0 μg/mL, detection range 15.6−500 μg/mL, and both intra-assay and interassay CV < 15%; The bovine KNG1 ELISA used for validation is a quantitative sandwich ELISA with a analytical sensitivity of 0.1 ng/mL, detection range 0.5−16 ng/mL and intra-assay and interassay CVs are <15%; The bovine LBP ELISA kit has a lower limit of detection of 0.233 ng/mL, detection range 0.625−40 ng/mL, no cross reactivity between LBP and other analogues observed with an intra-assay CV < 10% and interassay CV < 12%. The microtiter plate provided is precoated with an antibody specific to LBP and uses a biotin-conjugated antibody preparation specific to LBP. The information provided about the specific antibodies used in these kits by the manufacturer is limited, so it was not possible to further validate the kits.

Standards and blanks were analyzed in duplicate, while one single well was analyzed for the rest of the samples. For optimization, various dilutions of the sera were tested and the final dilution was determined as 1:20, 1:3, 1:2, 1:3, 1:5, and 1:5 for ELISA kits for IGFBP2, ORM1, CFH, SERPINC1, KNG1, and LBP, respectively. The mean value of the blank control was subtracted from the raw optical density (OD) values, and then a standard curve was generated by plotting the absorbance on the horizontal X-axis and the corresponding protein concentration of each standard on the vertical Y-axis using CurveExpert Professional 2.6.5 software. A 4-parameter Morgan-Mercer-Flodin (MMF) equation provided the best fitting ($r^2 > 0.99$ in all the ELISAs performed) between the average OD of each standard and its concentration. Finally, the concentration of the selected proteins in each sample was interpolated from the equation.

2.5. Statistical Analysis

Statistical analysis was performed using the R program[52] version 4.1.2 (https://www.r-project.org/). The pROC and Optimal Cutpoints packages of the R Program with confidence intervals (CI) stated at 95% were used for the Receiver operator characteristic (ROC) curve analysis. ROC analysis was used to determine the area under the curve (AUC) and the optimal cutoff value for each comparison. Optimal cutoff values for sensitivity and specificity were based on the maximum Youden Index (J = Se + Sp-1). The discriminatory power of the ELISAs to discern between the different experimental groups was considered as follows:[38,53] AUC values ≥ 0.9 were considered to

https://doi.org/10.1021/acs.jproteome.3c00244
J. Proteome Res. 2024, 23, 2762−2779

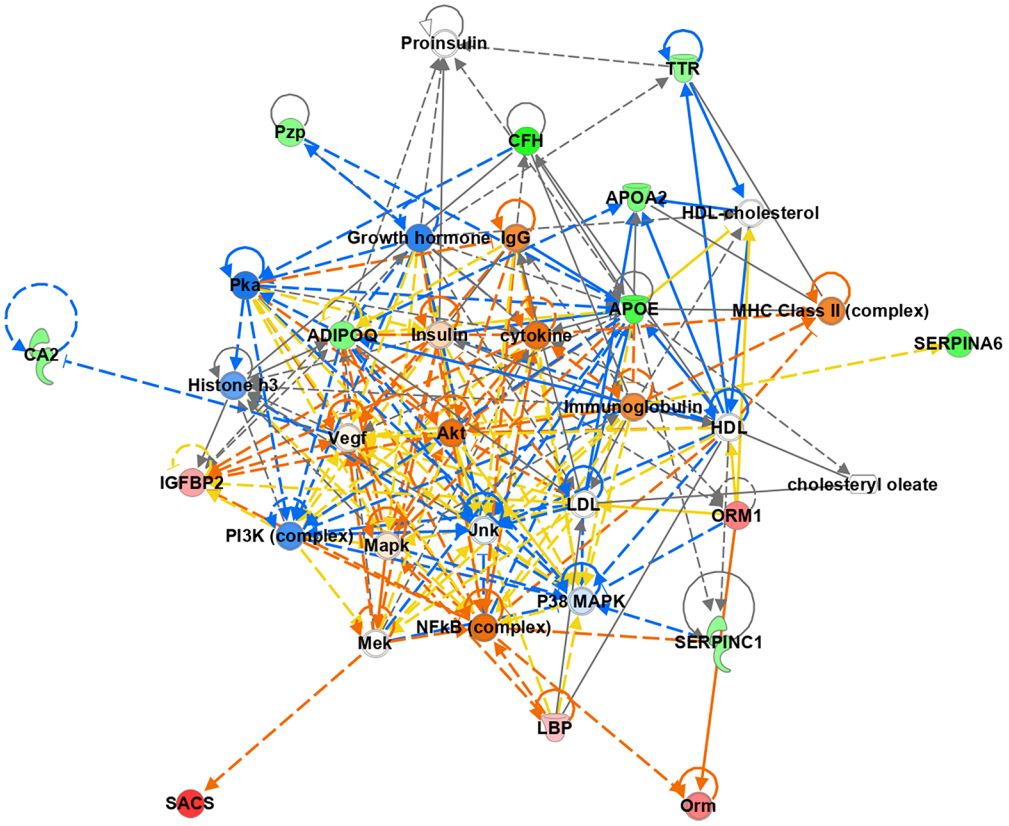

Figure 1. Functional clustering of differentially abundant proteins in serum of animals with focal lesions versus control animals using Ingenuity Pathway Analysis (IPA). The top network "Lipid Metabolism, Molecular Transport and Small Molecule Biochemistry" (score 37) with the main protein-to-protein interactions is represented. Activation of cytokines, IgGs, immunoglobulins, protein kinase B (Akt), and the nuclear factor kappa β (NFKB) complex are predicted. Upregulated proteins are shown in red, and downregulated proteins in green (light red and green indicate less extreme increased or decreased measurement in the data set). Orange indicates the prediction of activation of a pathway and blue prediction of inhibition (lighter orange and blue indicate that the prediction has been done with less confidence). Solid lines indicate direct connections, while dotted lines indicate indirect connections (circular arrows mean influence itself). The pointed and blunt arrowheads represent activating and inhibitory relationships, respectively. Orange lines indicate activation, blue inhibition, yellow indicates that findings are inconsistent with the state of downstream molecule, and gray indicates no predicted effect.

have excellent discriminatory power; $0.8 \leq$ AUC < 0.9 good discriminatory power; $0.7 \leq$ AUC < 0.8 fair discriminatory power; and AUC < 0.7, poor discriminatory

The differences in quantitative variables between two groups were studied with the *t* test of Student or Wilcoxon test for independent samples, depending on whether the hypothesis of normality was verified. If the groups to be compared were more than 2, the ANOVA test or the test of Kruskal–Wallis was used according to whether the hypotheses of normality and/or homoscedasticity were fulfilled. Tukey or Dunn tests were used for posthoc pairwise comparisons. The significance level was set at 0.05.

The simultaneous combination of 6 and 2 biomarkers is proposed in order to obtain a better prognosis of the lesion, compared to the use of a single biomarker. For this purpose, a multivariate binary logistic regression model, including the six biomarkers as predictors, was constructed, and the estimated probability was calculated. Afterwards, individuals with predicted probability equal to or greater than 0.5 are classified as with lesions, and those with lower values (<0.5) without lesions. The confusion matrix built from these values predicted by the model, together with the observed values, allows us to obtain the sensitivity and specificity of the chosen combination of biomarkers, and the AUC values. The model was constructed for the comparisons with more interest from a diagnosis point of view (focal vs control and all lesions vs control). In order to save costs, a model with 2 biomarkers was also built.

3. RESULTS

3.1. Quantitative Proteomic Analysis

TMT-6plex quantitative proteomics was used to analyze samples from three groups of animals (focal, diffuse, and control). Combining the information obtained from the four search engines (Mascot Server v2.5.1, OMSSA, X! TANDEM, and Myrimatch) against the *Bos taurus* protein database (UniProt knowledgebase), 669 proteins were identified (FDR < 1%) belonging to 333 protein groups. Three hundred and eighty-three quantification groups were detected; however, due to the high intraheterogenicity found within the three animal groups, only one (focal vs. control), eight (diffuse vs. control), and four (focal vs. diffuse) DA bovine proteins were detected with a *q*-value < 0.05 (Table 3). ORM1 was found to be upregulated in animals with focal and diffuse lesions vs. control animals (*q*-value < 0.01), while FETUB, IGFBP2, GC, complement component 6 (C6), and Sacsin molecular chaperone (SACS) were found to be upregulated in animals with diffuse lesions (*q*-value < 0.05). Serpin domain-containing protein (*q*-value < 0.01) and serum amyloid A (SAA) (*q*-value < 0.05) were downregulated in animals with diffuse lesions vs

https://doi.org/10.1021/acs.jproteome.3c00244
J. Proteome Res. 2024, 23, 2762−2779

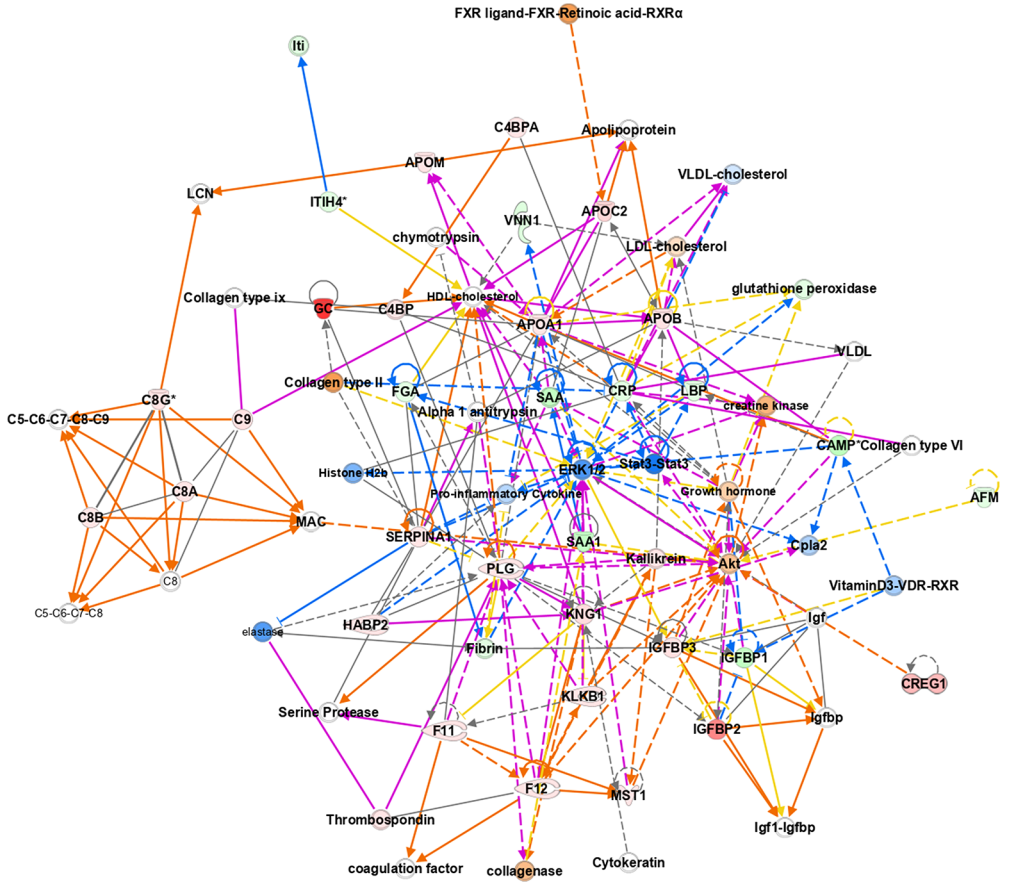

Figure 2. Functional clustering of differentially abundant proteins in serum of animals with diffuse lesions *versus* control animals using Ingenuity Pathway Analysis (IPA). Merged networks 1 and 2 (network 1. Humoral immune response, Inflammatory response, Hematological system development and function (score 31); and network 2. Inflammatory response, Organismal injury and abnormalities, Cell death and survival (score 31)) with four main nodes (complement system, the blood coagulation/anticoagulation cascade, metabolism of lipids and carbohydrates) are represented. Upregulated proteins are shown in red, and downregulated proteins are in green (light red and green indicate less extreme increased or decreased measurement in the data set). Orange indicates the prediction of activation of a pathway and blue prediction of inhibition (lighter orange and blue indicate that the prediction has been done with less confidence). Solid lines indicate direct connections, while dotted lines indicate indirect connections (circular arrows mean influence itself). The pointed and blunt arrowheads represent activating and inhibitory relationships, respectively. Orange lines indicate activation, blue inhibition, yellow indicate that findings are inconsistent with the state of downstream molecule, and gray indicates no predicted effect.

control animals. LPB and Serpin domain-containing protein were found to be upregulated (q-value < 0.01), and carbonic anhydrase 2 (CA2) (q-value < 0.01) and kininogen 2 (q-value < 0.05) were downregulated in animals with focal lesions vs. animals with diffuse lesions. This finding suggest that these proteins may be of interest for differential diagnosis.

In order to obtain information about the biological processes enriched in animals with PTB-associated focal and diffuse histological lesions, IPA analysis was performed including the list of all the DA proteins in the categories confident, likely, and putative (1 confident and 18 putative proteins for the focal vs control comparison; 3 confident, 1 likely, and 45 putative for the focal vs. diffuse; and 3 confident, 5 likely, and 105 putative proteins for diffuse vs. control comparison). Functional enrichment analysis using IPA of the DA proteins in the focal vs. control comparison identified two top networks with the following main associated functions: network (1) Lipid Metabolism, Small Molecule Biochemistry, Cell-to-cell signaling and interaction (score 37) (Figure 1) and network (2) Cancer, Organismal injury and abnormalities, Tumor morphology (score 9). Network (1), with upregulation of the IGBF2, SACS, LBP, and ORM1 and downregulation of apolipoprotein A-II (APOA2), apolipoprotein E (APOE), adiponectin (ADIPOQ), alpha-2-macroglobulin like (PZP), TTR, serpin Family A member 6 (SERPINA6), SERPINC1, and CA2, predicts activation of cytokines, IgGs, Immunoglobulins, protein kinase B (Akt) and the nuclear factor kappa β (NFKB) complex. The predicted alterations in carbohydrates and lipid metabolism, immune response, and inflammation may be essential processes in early stages of PTB.

Five top networks were generated in the diffuse vs. control comparison: network (1) Humoral immune response, Inflammatory response, Hematological system development and function (score 31); network (2) Inflammatory response, Organismal injury and abnormalities, Cell death and survival (score 31); network (3) Cell-to-cell signaling and interaction, Cell death and survival, Hematological system development and function (score 29); network (4) Cell morphology, Cellular movement, Hematological system development and function (score 17); and network (5) Developmental disorder, Hereditary disorder, Immunological disease, (score 12). Figure 2 represents merged networks (1) and (2) with four main nodes observed related to (1) the complement system with 6 upregulated proteins (CFH, complement component C7

https://doi.org/10.1021/acs.jproteome.3c00244
J. Proteome Res. 2024, 23, 2762−2779

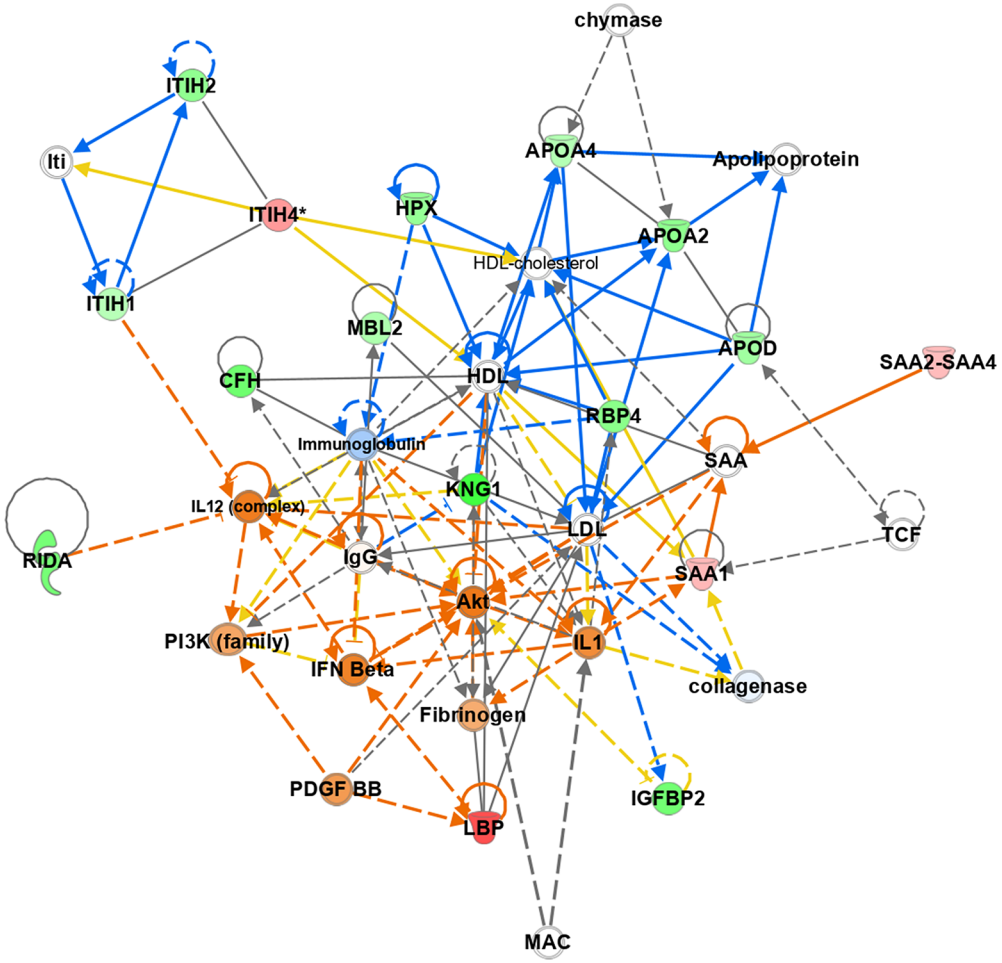

Figure 3. Functional clustering of differentially abundant proteins in serum of animals with focal lesions *versus* diffuse animals using Ingenuity Pathway Analysis (IPA). The top network "Carbohydrate metabolism, Lipid metabolism, Molecular transport" (score 41) with the main protein-to-protein interactions is represented. Alterations in the immune response and lipid metabolism related to the disease stage are observed. Upregulated proteins are shown in red, and downregulated proteins are in green (light red and green indicate less extreme increased or decreased measurement in the data set). Orange indicates the prediction of activation of a pathway and blue prediction of inhibition (lighter orange and blue indicate that the prediction has been done with less confidence). Solid lines indicate direct connections, while dotted lines indicate indirect connections (circular arrows mean influence itself). The pointed and blunt arrowheads represent activating and inhibitory relationships, respectively. Orange lines indicate activation, blue inhibition, yellow indicates that findings are inconsistent with the state of downstream molecule, and gray indicates no predicted effect.

(C7), C6, complement C8 alpha chain (C8A), complement component 8 subunit beta (C8B) and Complement component C9 (C9)); (2) the blood coagulation/anticoagulation cascade with 8 up-regulated proteins (thrombospondin, coagulation factor XI (F11), coagulation factor XII (F12), plasminogen (PLG), hyaluronan-binding protein 2 (HABP2), KNG1, plasma kallikrein (KLKB1), hepatocyte growth factor-like protein (MST1)); (3 and 4) metabolism of lipids and carbohydrates standing out the upregulation of IGFBP2, insulin-like growth factor-binding protein 3 (IGFBP3), apolipoprotein A-I (APOA1) and apolipoprotein C-II (APOC2) and down-regulation of insulin-like growth factor-binding protein 1 (IGFBP1), LBP, serum amyloid A1 (SAA1), serum amyloid A4 (SAA4), and pyruvate kinase M (PKM).

As the disease progresses, DA proteins give rise to alterations in different biological functions or physiological processes shown in the three top networks generated by IPA when focal vs diffuse animals are compared: network (1) Carbohydrate metabolism, Lipid metabolism, Molecular transport (score 41) (Figure 3); network (2) Infectious diseases, Organismal injury and abnormalities, Developmental disorder (score 29); and network (3) Cardiovascular disease, Hematological disease, Organismal injury and abnormalities (score 10). When we compare the two stages of the disease upregulation of LBP and downregulation of IGFBP2, KNG1, APOA2, apolipoprotein A-IV (APOA4), apolipoprotein D (APOD) and CFH are observed revealing alterations in the immune response and lipid metabolism.

Table 4 shows the five top canonical pathways and five top diseases and disorders affected by PTB progression. Moreover, the differences observed between the top networks, functional categories, and diseases identified by IPA for the focal vs diffuse comparison are indicative of disease progression produced by alterations at the molecular level that mainly affect the metabolism of lipids and sugars, acute-phase response signaling, complement system, and coagulation cascade.

3.2. Validation of Differentially Abundant Proteins by ELISA

Following an integrated analysis of proteomics and functional results considering the fold change (log2 fold change), cellular localization (preference for secreted proteins), biological function (association with immune and inflammatory responses) and availability of specific immunological tools for

https://doi.org/10.1021/acs.jproteome.3c00244
J. Proteome Res. 2024, 23, 2762−2779

Table 4. Top 5 Canonical Pathways and Diseases and Disorders Related to Animals with Paratuberculosis (PTB)-Associated Focal and Diffuse Histological Lesions[a]

animals with focal histological lesions (focal vs. control)		animals with diffuse histological lesions (diffuse vs control)		focal vs. diffuse	
top canonical pathways	−Log (*p*-value)	Top canonical pathways	−Log (*p*-value)	top canonical pathways	−Log (*p*-value)
LXR/RXR activation	7.83	LXR/RXR activation	30.64	Acute Phase Response signaling	15.25
Acute Phase Response signaling	6.94	FXR/RXR activation	30.41	LXR/RXR activation	13.27
FXR/RXR activation	5.87	Acute Phase Response signaling	28.48	FXR/RXR activation	11.30
Maturity onset diabetes of young (MODY) signaling	4.70	Coagulation system	19.28	Complement system	6.75
Atherosclerosis signaling	4.03	Complement system	16.80	Clathrin-mediated endocytosis signaling	5.08
diseases and disorders	-Log (p-value) range	Diseases and disorders	−Log (*p*-value) range	diseases and disorders	−Log (*p*-value) range
Inflammatory response	2.60−6.60	Cardiovascular disease	5.71−26.73	Infectious diseases	2.87−13.10
Endocrine system disorders	2.57−5.67	Hematological disease	6.01−26.73	Organismal injury and abnormalities	2.39−13.10
Gastrointestinal disease	2.57−5.67	Organismal injury and abnormalities	5.69−26.73	Inflammatory response	2.39−10.44
Metabolic disease	2.57−5.67	Infectious diseases	5.75−24.31	Renal and Urological Disease	2.39−8.56
Organismal injury and abnormalities	2.57−5.67	Inflammatory response	5.77−23.00	Cardiovascular disease	2.40−7.07

[a]LXR, RXR, and FXR refer to Liver X Receptors, Retinoid X Receptors, and Farnesoid X Receptor, respectively.

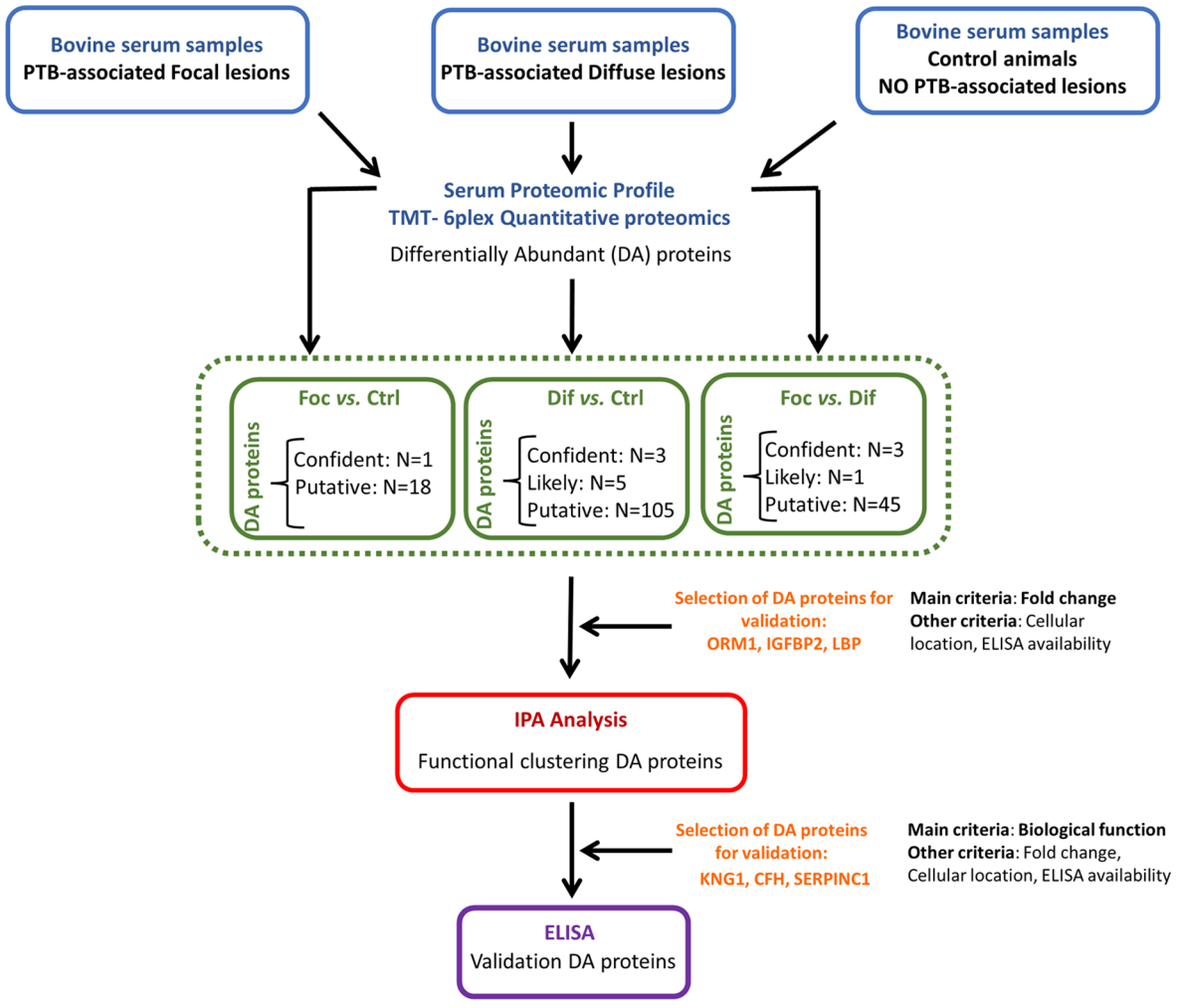

Figure 4. Flowchart showing the analysis of bovine plasma by TMT-6plex quantitative proteomics and selection of differentially abundant proteins for validation. IPA, Ingenuity Pathway Analysis; IGFBP2, bovine insulin-like growth factor binding protein 2; ORM1, alpha-1-acid gycoprotein1; CHF, complement factor H; SERPINC1, bovine anti-thrombin III; KNG1, kininogen 1; and LBP, lipopolysaccharide binding protein.

https://doi.org/10.1021/acs.jproteome.3c00244
J. Proteome Res. 2024, 23, 2762−2779

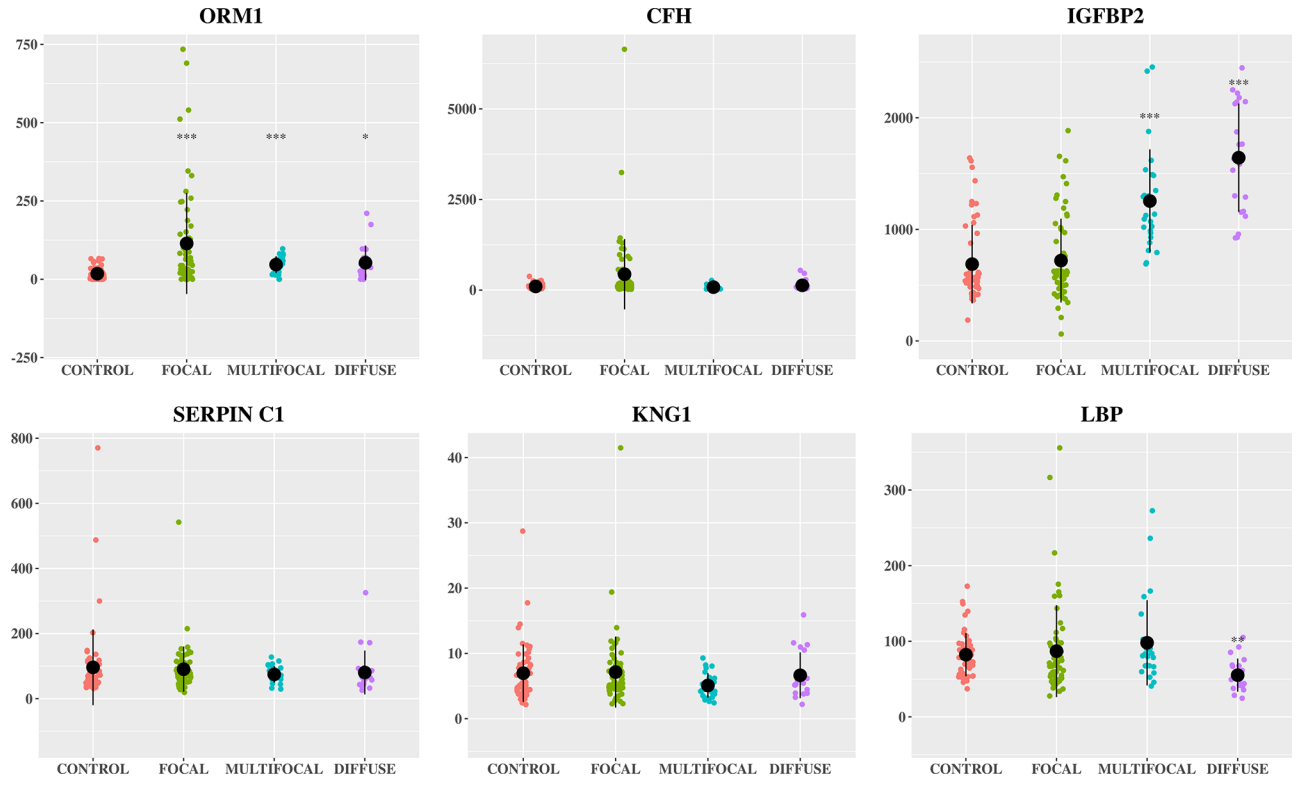

Figure 5. Serum levels of ORM1, CFH, IGFBP2, SERPINC1, KNG1, and LBP in Holstein Friesian cows with focal (n = 61), multifocal (n = 25) , and diffuse (n = 22) histopathological forms of bovine paratuberculosis (PTB) and negative control animals from PTB-free farms (n = 56). The protein concentrations were quantified by specific ELISAs supplied by MyBioSource, San Diego, CA, USA. Data are represented in scatter plots with each dot representing a single animal. The mean value of each histopathological group is represented by a gross black point and the standard deviation by a vertical line. The concentrations are expressed in μg/mL for SERPINC1 and ng/mL for IGFBP2, ORM1, CFH, KNG1, and LBP (Y-axis). IGFBP2, bovine insulin-like growth factor binding protein 2; ORM1, alpha-1-acid gycoprotein1; CFH, complement Factor H; SERPINC1, bovine anti-thrombin III; KNG1, kininogen 1; and LBP, lipopolysaccharide binding protein. The asterisks indicate that differences between each histopathological group and the control are significant (* $p < 0.05$, ** $p < 0.01$, *** $p < 0.001$).

Table 5. IGFBP2, ORM1, CFH, SERPINC1, KNG1, and LBP Mean Concentration Values in the Different Histopathological Groups and in the Paratuberculosis (PTB)-free Control Group[a]

histological group	IGFBP2	ORM1	CFH	SERPIN C1	KNG1	LPB
FOCAL (n = 61)	719.99 ± 375.81	114.29 ± 161.33***	436.86 ± 969.23	90.59 ± 69.54	7.14 ± 5.44	86.95 ± 60.80
MULTIFOCAL (n = 25)	1253.86 ± 463.18***	46.74 ± 26.75***	80.42 ± 53.68	74.70 ± 24.89	5.09 ± 1.89	98.02 ± 56.38
DIFFUSE (n = 22)	1642.34 ± 485.79***	52.58 ± 55.15*	130.99 ± 141.89	80.43 ± 67.39	6.65 ± 3.51	55.20 ± 21.86***
ALL (n = 108)	1031.46 ± 563.22***	86.09 ± 128.06***	295.08 ± 754.25**	84.84 ± 61.55	6.57 ± 4.55	83.51 ± 55.89
PTB-FREE CONTROL (n = 56)	688.54 ± 351.77	17.67 ± 19.63	100.05 ± 66.19	96.34 ± 116.37	6.97 ± 4.40	82.25 ± 28.53

[a]IGFBP2, bovine insulin-like growth factor binding protein 2; ORM1, alpha-1-acid gycoprotein1; CFH, complement factor H; SERPINC1, bovine anti-thrombin III; KNG1, kininogen 1; LBP, lipopolysaccharide binding protein; ALL, includes animals with focal, multifocal, and diffuse lesions. The concentrations are expressed as the mean value of the group ± standard deviation (SERPINC1 in μg/mL and IGFBP2, ORM1, CFH, KNG1, and LBP in ng/mL). The asterisks indicate that differences between each histopathological group and the control are significant (* $p < 0.05$, ** $p < 0.01$, *** $p < 0.001$).

their detection, six DA proteins (IGFBP2, ORM1, CFH, SERPINC1, KNG1, and LBP) included in the top associated resulting IPA networks and functional categories were selected as candidates to be validated by ELISA in order to confirm the proteomic results and to investigate their potential as PTB biomarkers. IPA analysis suggested that KNG1, CFH, and SERPINC1 may be modulators of the inflammatory response. Figure 4 shows the flowchart of the study and the criteria used for the selection of the DA proteins to be validated.

In order to validate the proteomic results, the serum concentration of these proteins was investigated by ELISA using a relatively large set of reference samples from 108 infected animals with focal (n = 61), multifocal (n = 25), and diffuse lesions (n = 22) and 56 control animals from PTB-free farms (see Table 2 and Supplementary Table 1). The concentrations of the six selected proteins in each individual serum sample are shown in Figure 5, and the mean values of the concentrations for each animal group are shown in Table 5. The trends of the serum expression levels of the selected DA proteins results were quite consistent with the proteomic results (Tables 3 and 5). In agreement with the proteomic results: IGFBP2 serum levels were significantly increased in the multifocal, diffuse, and all type of lesions groups with respect to the PTB-free control group ($p <$ 0.001 in all cases), slightly increased in the focal with respect to

https://doi.org/10.1021/acs.jproteome.3c00244
J. Proteome Res. 2024, 23, 2762−2779

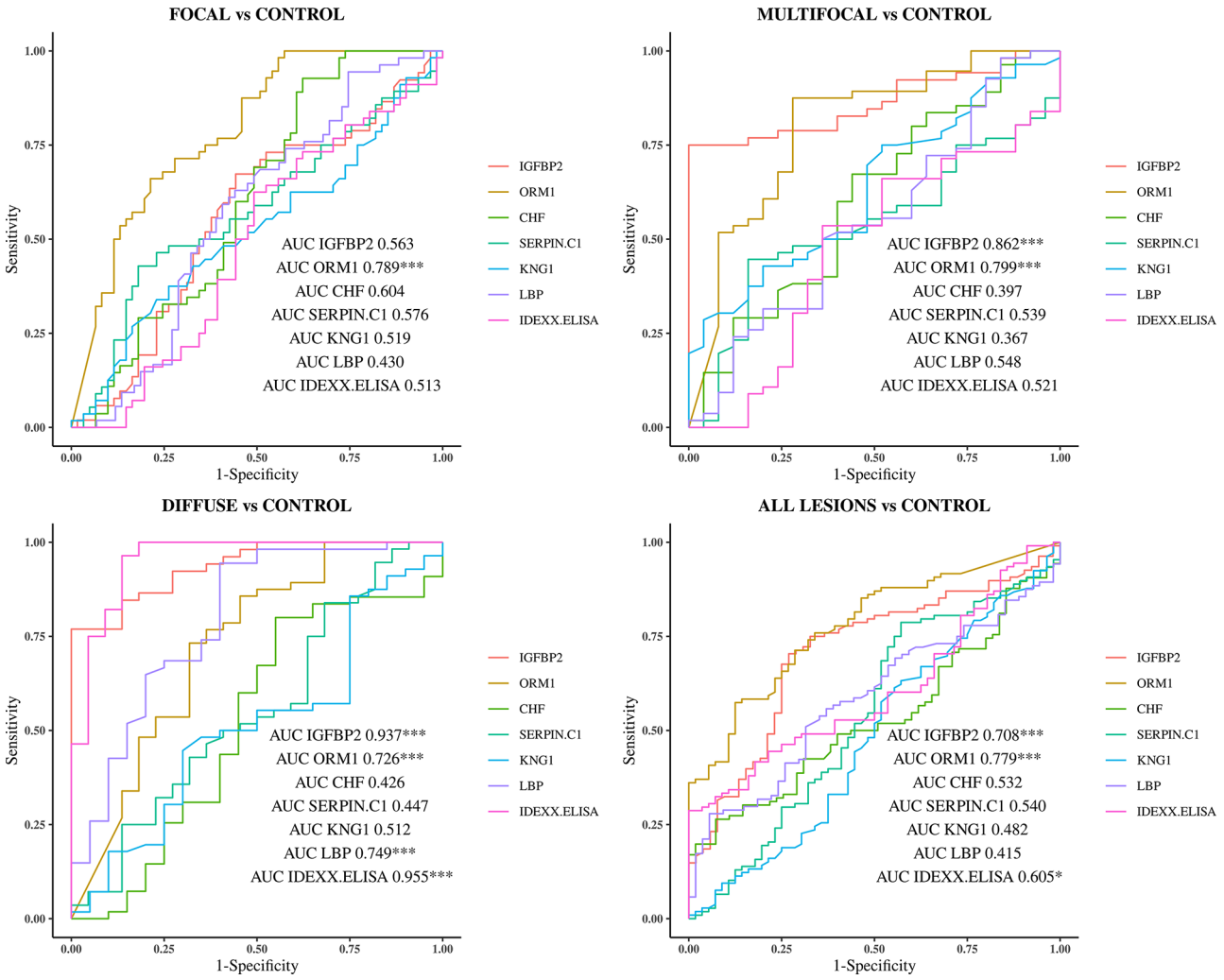

Figure 6. Receiver operator characteristic curves (ROC curves) analysis of the IGFBP2, ORM1, CFH, SERPINC1, KNG1, and LBP bovine proteins-based ELISA' results of serum samples from Holstein Friesian cows with focal ($n = 61$), multifocal ($n = 25$), and diffuse ($n = 22$) pathological forms of bovine paratuberculosis (PTB) and negative control animals from PTB-free farms ($n = 56$). All, includes animals with focal, multifocal, and diffuse lesions; vs, versus; IGFBP2, bovine insulin-like growth factor binding protein 2; ORM1, alpha-1-acid gycoprotein1; CFH, complement Factor H; SERPINC1, bovine anti-thrombin III; KNG1, kininogen 1; and LBP, lipopolysaccharide binding protein. The asterisks indicate that a specific ELISA detects significant differences (* $p < 0.05$, ** $p < 0.01$, *** $p < 0.001$) between the compared histopathological groups.

the control ($p = 0.649$), and significantly decreased in the focal with respect to the multifocal and diffuse groups ($p < 0.001$); ORM1 serum levels were significantly increased between all the considered histological groups and the control ($p < 0.001$ for the focal vs control, multifocal vs. control and all type of lesions vs control comparisons and $p < 0.05$ for the diffuse vs. control comparison); LBP serum levels were significantly increased in the multifocal vs. diffuse ($p = 0.001$), control vs diffuse ($p = 0.001$), and focal vs. diffuse ($p = 0.016$) group, and no significant differences were observed in the LBP serum levels of the focal vs. control, multifocal vs. control and focal vs. multifocal ($p > 0.05$) and all type of lesions vs control ($p = 0.852$); no significant differences in the serum levels of the "putative" SERPINC1 (log2-fold change −0.759 q-value 0.342) and KNG1 (log2 fold change 0.861 and q-value 0.334) proteins were observed between the different groups. Regarding CFH in contrast with the proteomic results (a putative protein downregulated in animals with focal lesions, log2 fold change −0.759, q-value 0.342) significant upregulation was observed when all lesioned animals vs control (p = 0.009) and multifocal vs focal ($p = 0.029$) animals were compared.

3.3. Evaluation of the Diagnostic Performance of the Differentially Abundant Selected Proteins-Based ELISAs

ROC analysis was carried out to evaluate the diagnostic performance of the IGFBP2, ORM1, CFH, SERPINC1, KNG1, and LBP-based ELISAs (Figure 6 and Table 6). In addition, the diagnostic performance of the candidate biomarker-based ELISAs was compared to that of the anti-Map ELISA, the most popular test used to detect Map-specific antibodies in exposed or infected animals. The AUC values of the IGFBP2, ORM1, CFH, SERPINC1, KNG1, and LBP-based ELISAs were 0.56, 0.79, 0.60, 0.58, 0.52, 0.43, and 0.51, respectively, when comparing the focal and the PTB-free control group, indicating that only the ORM1-based ELISA can discriminate between both groups ($0.7 \leq AUC < 0.8$ fair discriminatory power). The AUC values of the IGFBP2, ORM1, CFH, SERPINC1, KNG1 and LBP-based ELISAs were 0.86, 0.80, 0.40, 0.54, 0.37, 0.55 and 0.52, respectively, when comparing the multifocal and the control groups, indicating that the IGFBP2-based ELISA had the best ability to differentiate both groups, followed by the ORM1 protein (0.8

https://doi.org/10.1021/acs.jproteome.3c00244
J. Proteome Res. 2024, 23, 2762−2779

Table 6. Diagnostic Performance of the Six Differentially Abundant Protein-Based ELISAs to Detect Animals with Different Pathological Forms of Paratuberculosis and Comparison with the Anti-Map ELISA[a]

contrasts	ELISA	AUC	*p*-value	cut off	SE (%)	SP (%)	DV
Focal vs Control	IGFBP2	0.563	0.253	593.5	55.74	67.31	0.615
	ORM1	**0.789**	**<0.001**	**20.18**	**78.69**	**66.07**	**0.724**
	CFH	0.604	0.054	179.35	37.70	92.73	0.652
	SERPINC1	0.576	0.160	52.68	81.96	42.86	0.624
	KNG1	0.519	0.723	4.74	73.78	37.50	0.556
	LBP	0.430	0.201	97.43	27.12	83.33	0.552
	Anti-Map^{A}	0.513	0.804	28.39	14.75	100.00	0.574
	Anti-Map^{B}			55.00	6.56	100.00	0.533
	Fecal bacteriological culture				4.92	100.00	0.525
	Fecal PCR				11.48	100.00	0.557
Multifocal vs Control	**IGFBP2**	**0.862**	**<0.001**	**690.34**	**100.00**	**75.00**	**0.875**
	ORM1	0.799	<0.001	39.46	72.00	87.5	0.798
	CFH	0.397	0.142	266.44	4.00	98.18	0.511
	SERPINC1	0.536	0.606	54.47	84.00	44.64	0.643
	KNG1	0.367	0.057	2.43	100.00	1.79	0.509
	LBP	0.548	0.499	159.06	16.00	98.15	0.571
	Anti-Map^{A}	0.521	0.763	1.50	100.00	16.07	0.580
	Anti-Map^{B}			55.00	16.00	100.00	0.580
	Fecal bacteriological culture				8.00	100.00	0.540
	Fecal PCR				32.00	100.00	0.660
Diffuse vs Control	IGFBP2	0.937	<0.001	924.11	100.00	76.92	0.885
	ORM1	0.726	0.002	25.71	68.18	73.21	0.707
	CFH	0.479	0.787	283.86	15.00	98.18	0.566
	SERPINC1	0.447	0.474	53.08	63.64	42.86	0.533
	KNG1	0.512	0.878	5.15	70.00	44.64	0.573
	LBP	0.794	<0.001	50.62	60.00	94.44	0.772
	Anti-Map^{A}	**0.955**	**<0.001**	**19.6**	**86.36**	**96.43**	**0.914**
	Anti-Map^{B}			55.00	77.27	100.00	0.886
	Fecal bacteriological culture				27.27	100.00	0.636
	Fecal PCR				72.73	100.00	0.864
All Lesions vs Control	IGFBP2	0.708	<0.001	616.27	70.37	73.08	0.717
	ORM1	**0.779**	**<0.001**	**37.53**	**57.4**	**87.5**	**0.725**
	CFH	0.532	0.513	179.35	26.41	92.73	0.596
	SERPINC1	0.540	0.398	52.68	78.7	42.86	0.608
	KNG1	0.482	0.706	4.88	63.21	42.86	0.530
	LBP	0.415	0.081	159.06	10.58	98.15	0.544
	ANTI-MAP^{A}	0.598	0.027	20.76	27.78	100.00	0.639
	ANTI-MAP^{B}			55.00	19.44	100.00	0.597
	Fecal bacteriological culture				10.19	100.00	0.551
	Fecal PCR				28.70	100.00	0.644

[a]Six DA proteins were selected to be validated by ELISA, using a set of reference samples from 108 infected animals with focal (n = 61), multifocal (n = 25), and diffuse lesions (n = 22) and 56 control animals from PTB-free farms. ROC analysis of the ELISA results was performed to determine the AUC, sensitivity, and specificity values of each ELISA. AUC, area under the curve; *p*-value, *p*-value of the AUC area, indicates whether the discrimination between animals with focal, multifocal, diffuse, or with any type of lesion and the control animals is significant or not; cut-off point is expressed μg/mL for SERPINC1 and ng/mL for IGFBP2, ORM1, CFH, KNG1, and LBP, and indicates the DA proteins concentration above which an animal is considered positive; Se, sensitivity; Sp, specificity; DV, diagnostic value (semisum of sensitivity and specificity); vs, versus; IGFBP2, bovine insulin-like growth factor binding protein 2; ORM1, alpha-1-acid gycoprotein1; CHF, complement factor H; SERPINC1, bovine anti-thrombin III; KNG1, kininogen 1; and LBP, lipopolysaccharide binding protein; Anti-Map^{A}, anti-Map serum ELISA using the cutoff value calculated by ROC analysis; Anti-Map^{B}, anti-Map ELISA using the cutoff value established by the supplier. In bold face are shown the techniques with the best discriminatory power (higher AUC value) for each contrast.

≤ AUC < 0.9 good discriminatory power in both cases). Regarding the ability to discriminate between the diffuse and the control groups, the best diagnostic performance was for the anti-Map ELISA (AUC = 0.96) followed by the IGFBP2, LBP, and ORM1-based ELISAs with AUC values of 0.94, 0.79, and 0.73, respectively. The best discriminatory power for global detection of animals with any type of histological lesions was for the ORM1 (AUC 0.78, 57.40% sensitivity, and 87.50 specificity) and the IGFBP2 (AUC 0.71, 70.37% sensitivity and 73.08% specificity)-based ELISAs, while the anti-Map ELISA had a poor AUC value (0.61), 28.70% sensitivity, and 100% specificity for global detection. The performance of these ELISAs was also compared to that of the fecal bacteriological culture and real time PCR observing lower diagnostic values of the conventional diagnostic methods for the different histopathological groups (Table 6).

The multivariate binary logistic regression model constructed predicts that the combined use of six or two biomarkers

https://doi.org/10.1021/acs.jproteome.3c00244
J. Proteome Res. 2024, 23, 2762−2779

Table 7. Multivariate Binary Logistic Regression Models Including Six and Two Biomarkers as Predictors to Estimate the Probability of Animals Having Focal Lesions or Any Type of Lesion (All Lesions)[a]

contrasts	protein	coefficient	*p*-value	OR (CI 95%)	LRT	AUC	SE (%)	SP (%)
Focal vs Control				Complete model with 6 candidate biomarkers				
	IGFBP2	−0.001	0.078	0.998 (0.997−1.001)	<0.001	0.839	76.47	67.8
	ORM1	0.052	<0.001	1.054 (1.031−1.085)				
	CFH	−0.003	0.022	0.997 (0.994−1.001)				
	SERPINC1	−0.006	0.259	0.994 (0.981−1.002)				
	KNG1	0.159	0.057	1.173 (1.012−1.406)				
	LBP	0.008	0.133	1.008 (0.999−1.022)				
				Simplified model with 2 candidate biomarkers				
	ORM1	0.036	<0.001	1.037 (1.019−1.059)	<0.001	0.798	78.18	57.38
	CFH	−0.002	0.189	0.998 (0.996−1.003)				
All Lesions vs Control				Complete model with 6 candidate biomarkers				
	IGFBP2	0.001	0.0103	1.001 (1.001−1.002)	<0.001	0.841	64.71	82.69
	ORM1	0.041	<0.001	1.041 (1.024−1.064)				
	CFH	−0.002	0.0342	0.997 (0.995−1.001)				
	SERPINC1	−0.002	0.5529	0.998 (0.990−1.004)				
	KNG1	0.068	0.3035	1.070 (0.949−1.234)				
	LBP	0.004	0.3293	1.004 (0.996−1.014)				
				Simplified model with 2 candidate biomarkers				
	IGFBP2	0.001	0.004	1.001 (1.001−1.002)	<0.001	0.829	65.38	84.26
	ORM1	0.035	<0.001	1.035 (1.019−1.055)				

[a]The coefficients of the logistic regression model, significance (*p*-value), and odds ratio (OR) with the 95% confidence interval are shown. The goodness of fit of the model to predict lesions was evaluated with the likelihood ratio test (LRT). The area under curve (AUC), sensibility (SE), and specificity (SP) of the models are provided. VS, versus.

increases the diagnostic performance of the individual biomarkers-based ELISAs for global detection of animals with any type of lesion (see Tables 6 and 7). Thus, combination of two of these biomarkers (IGFBP2 and ORM1) gives an AUC of 0.829, sensitivity of 65.38%, and specificity of 84.26%. In the case of detection of animals with focal lesions, the diagnostic performance of the individual biomarkers-based ELISAs is lower than the combination of the six biomarkers (AUC 0.839, sensitivity 76.47%, and specificity 67.80%). However, the combination of two biomarkers (ORM1 and CFH) with an AUC value of 0.798, sensitivity 78.18%, and specificity of 57.38% does not improve the results obtained with the ORM1-based ELISA. The sensitivities of both the individual biomarkers and the combined models are higher than those of conventional methods such as fecal culture, fecal PCR, and anti-Map ELISA (see Tables 6 and 7).

4. DISCUSSION

To the best of our knowledge, this is the first study that investigates the serum proteomic profiles of Holstein Friesian cows infected with Map in relation to the different histopathological forms (focal and diffuse) associated with PTB. The members of each established group (see Table 1), representing different stages of the disease, share the same type of histological lesion (focal, diffuse, or control); however, the age and specific infectious status of each animal within a group is different. This high intraheterogeneity might be responsible for the low number of DA bovine proteins with a *q*-value < 0.05 detected (Table 3) in the proteomic analysis. Seth et al. (2009)[24] found DA proteins, ORM1 and FETUB, to be elevated only in *M. bovis* but not in Map infected animals. ORM1 was included in a diagnostic model[45] designed to discriminate between latent and active TB. TTR, RBPs, and CATHL were found to be upregulated in both studies.[24,45] TTR has been also proposed as a putative serum biomarker of Map infection in sheep. IGFBP2, another interesting candidate biomarker, was upregulated in animals with diffuse lesions. Related proteins, such as IGFBP1 and IGFBP3, were found to be upregulated in Map-infected cattle and in pulmonary vs latent TB, respectively. Other studies[25] identified different proteins (TF, GSN isoforms alpha and β, C1R, C3, AOC3, F2, COAFXIII, and FGG and its precursor) as potential biomarkers of Map infection.

The predicted top networks, pathways, and diseases (Figures 1, 2, and 3 and Table 4) can be related to a chronic inflammatory infectious disease such as PTB. During infection and inflammation, a wide range of alterations occurs in metabolism.[54] These changes may be mediated by nuclear receptors activation such as Liver X Receptors (LXRs) and Farnesoid X Receptors (FXR). Both heterodimerize with the Retinoid X Receptors (RXR), regulating gene expression in response to ligands that can activate or suppress transcription affecting biological and pathological processes. LXRs have been shown to regulate expression of some important genes involved in lipid metabolism.[55,56] FXRs, on the other hand, play an important role in the regulation of the metabolism of carbohydrates, lipids, and inflammation.[57−59] FXRs also regulate APPs expression.[60] These APPs are part of the body's reaction known as the acute-phase response (APR). The APR induces changes in the concentration of specific plasma proteins.[61] The increase of positive APPs modulates the inflammatory response by directly neutralizing foreign agents, minimizing the extent of tissue damage, and participating in tissue regeneration. Likewise, alterations in the levels of cytokines, mediators of metabolic changes, are observed during infection and inflammation, which affect lipoprotein metabolism and produce changes in the plasma concentrations of lipids.[62]

These alterations in the APR and lipoproteins metabolism have been observed in our study (see Figures 1, 2, and 3). The APR signaling is one of the top canonical pathways affected by Map infection, which plays an important role in the

https://doi.org/10.1021/acs.jproteome.3c00244
J. Proteome Res. 2024, 23, 2762−2779

inflammatory process induced by Map (Table 4). Positive APPs, ORM1 and LBP, were found to be upregulated after Map infection, while negative APPs like SAA, SERPINC1, and TTR were downregulated. ORM1 is a widely used marker in inflammatory diseases.[63] ORM1 contributes to the general function of the APR as a coordinated system that modulates host immune responses during periods of intense inflammation and tissue destruction.

LBP classically plays a role mainly in the recognition patterns from Gram-negative bacteria but also of several bacterial surface patterns from Gram-positive bacteria.[64] LBP was found to bind glycolipids of *Mycobacteria* spp., thus stimulating mononuclear cells and macrophages.[65] At high concentrations (acute-phase levels), LPB can inhibit cell responses to bacterial patterns. Moreover, LBP can be also involved in the activation of p38 MAPK and NF-κB[66] which occupy central nodes of network 1 (Figure 1) and is involved in the upregulation of cytokines that lead to inflammation. If LPB levels increase, the host knows that something is wrong, so LPB activity is regulated by the direct binding of lipoproteins resulting in down-modulation of the inflammatory response. CFH, the primary regulator of the alternative complement pathway in plasma, is susceptible to similar situations. CFH can interact directly with APOE molecules, which may contribute to complement dysregulation in plasma.[67] Additionally, CFH can recognize specific markers on host cells and controlling complement on its own surfaces. Unfortunately, some pathogens exploit this property as an evasion strategy by binding directly to CFH,[68,69] thereby evading complement attack. Therefore, CFH may play a crucial role in evasion processes employed by Map. SERPINA6 and SERPINC1 are considered negative APPs[70] whose levels decrease during the APR. CFH and SERPINC1 may be modulators of the inflammatory response in early stages of PTB. Downregulation of SERPINC1 is associated with mycobacterial infections such as pulmonary TB in humans.[71] SERPINC1 may be also related to the expression of retinol-binding protein 4 (RBP4),[72] a potential biomarker of PTB.[24]

Espinosa et al. (2020)[73] observed variation of the APR (haptoglobin (HP) and SAA) between the different pathological forms of PTB according to the predominant immune response observed in each form. Thus, focal, multifocal, and diffuse paucibacillary lesions are associated with a Th1 cell-mediated immune response with a predominance of pro-inflammatory cytokines[74,75] which induce APPs production at the hepatic level. However, in animals with diffuse multibacillary lesions predominately a Th2 humoral immune response with the production of anti-inflammatory cytokines (IL4, IL10)[76] is responsible of the lack of hepatic stimulation consistent with the lower levels of APPs that they observed. These authors[73] hypothesize that APPs levels are higher in focal, multifocal, and diffuse paucibacillary types of lesions, where the presence in the tissues of acid-fast bacteria (AFB) is scarce, and lower in those lesions where there is a large number of AFB, indicating that both HP and SAA may contribute to the limitation of Map multiplication in the tissues of Map-infected cows. In agreement with these results, in our study (Tables 3 and 5), higher levels of APPs were found in animals with focal and multifocal than in animals with diffuse lesions (larger numbers of AFB), suggesting that APPs may play an important role in the control of Map.

As we mentioned before, alterations in lipoproteins metabolism are also related to infection and inflammation. The relationship between the host innate immunity and the serum composition of lipoproteins and lipids is well known. Thus, functional enrichment analysis using IPA revealed that hyperlipidemia and lipid and lipoprotein metabolism alterations begin to appear in the early stages of PTB (see Figures 1 and 3). These alterations might be mediated or mitigated by ORM1, which has been identified as a possible regulator of lipid[77] and carbohydrate metabolism.[78] This is consistent with the low levels of ADIPOQ.[79,80] In accordance with this, IPA analysis led to elucidate the importance of mechanisms involved in carbohydrates and their relationship with lipid disorders in PTB through the dysregulation of proteins involved in insulin response, biosynthesis, transport, and storage of lipids and lipoproteins (Figure 1).

In fact, insulin occupies one of the central nodes in Figure 1, where its predicted expression is upregulated. Insulin also plays an important role in regulating the transport of very low-density lipoprotein (VLDL).[81] Classical forms of insulin resistance are characterized by low ADIPOQ levels known as hypoadiponectinemia,[79,80] which we observed in our results (Figure 1). Alterations observed due to hypoadiponectinemia were also related to IGFBF2. IGFBP2 is one of six similar secreted proteins that binds insulin-like growth factors (IGF) IGF-I and IGF-II with high affinity. IGFBP2, which also interacts with other different ligands, is linked to cellular migration, growth, cell adhesion, and apoptosis. IGFBP2 can inhibit IGF-I and IGF-II actions;[82] the binding of IGFBP2 to IGF-I prevents IGF-1 linkage to its receptors, thereby contributing to modulating insulin sensitivity. In fact, IGFBP2 high concentrations reflect long-term insulin sensitivity.[83] IGFBP2 is involved in metabolic homeostasis, diabetes, and obesity, so it has been suggested to use IGFBP2 as a marker protein for cancer with metabolic dysfunction that conduces to malnutrition.[84] Recently, it has also been reported that overexpression of IGFBP3 increased proteolysis, inhibited myogenesis, and decreased muscle mass in pancreatic cancer-induced cachexia.[85] Upregulation of IGFPB3 is observed in our results in the last stages of PTB (see Figure 2), which is consistent with the progressive loss of weight and development of cachexia observed in those animals.

The joint analysis of proteomics and IPA results underlines the mechanisms by which the disease progresses. It is well accepted that Map-infected animals develop an initial Th1 cell-mediated immune response, which might control bacterial spread and result in either bacterial clearance or subclinical infection. This process may be triggered by production of IL-12 and IL-1 which are predicted to be overexpressed (Figure 3). However, in the clinical phase, animals exhibit a Th2 humoral immune response, which fails to contain the infection, where we observed activation of the complement system (see Figure 2). This process may begin at subclinical stages through IL-6 production predicted by IPA analysis in the focal vs control comparison (Z-value = 0.639) (data not shown). Clinical signs associated with PTB are absent in the subclinical stage, while advanced stages of the disease are characterized by severe enteritis with diarrhea, leading to wasting and gradual emaciation despite an uninfluenced feed uptake. The changes in lipid and carbohydrate metabolism mentioned above, limiting the delivery of fuel to the muscles for generation of energy and to the adipose tissues for storage of energy, contribute to the reduction of body mass observed in advanced PTB stages. Furthermore, our results show activated coagulation processes that could correspond to the high severity of PTB-diffuse lesions where arteritis and thrombus formation can be observed.[49] Accordingly, IPA's suggestion for the development of cardiovascular diseases seems to be correct (Table 4).

https://doi.org/10.1021/acs.jproteome.3c00244
J. Proteome Res. 2024, 23, 2762−2779

Good biomarkers must be specific, robust, and applicable to clinical use.[86] Our results showed that biomarker-based ELISAs could be useful diagnostic tools for the detection of subclinical infections, complementing conventional diagnostic methods. However, it is worth mentioning that the use of APPs, such as ORM1, as PTB-biomarkers has some drawbacks as the ELISAs based on the detection of these potential biomarkers can be highly sensitive but sometimes lack specificity as they are found to be elevated in other concurrent inflammatory diseases such as bovine respiratory disease, mastitis, and lameness.[87−92] IGFBP2 is a potential biomarker of PTB-associated metabolic disorder that would allow a more specific diagnosis. However, its association with these metabolic disorders in PTB should be further investigated. The establishment of adequate management protocols on farms incorporating the use of these biomarker-based ELISAs could help to reduce the prevalence of this costly and widespread disease.

■ ASSOCIATED CONTENT

Supporting Information

The Supporting Information is available free of charge at https://pubs.acs.org/doi/10.1021/acs.jproteome.3c00244.

Supplementary Table 1. Infectious status of all the animals used to validate the proteomic results and to investigate the potential of the selected proteins (IGFBP2, ORM1, CFH, SERPINC1, KNG1, and LBP) as paratuberculosis (PTB) biomarkers. Supplementary Figure 1. Scatter plot showing the correlation between the proteomic results (log2 fold change obtained for each identified protein) of experiments TMT-6plex pool 1 (TMT1) and pool II (TMT2) for both the Focal vs control (A) and diffuse vs. control (B) comparisons. Supplementary Figure 2. Volcano plots displaying the differentially abundant (DA) proteins identified by TMT-6plex quantitative proteomics analysis of serum of Holstein Friesian cows (confident (q-value < 0.01), likely (q-value < 0.05) and putative (q-value > 0.05 but p-value < 1-π0) proteins). Supplementary Figure 3. Volcano plots displaying the differentially abundant (DA) proteins identified by TMT-6plex quantitative proteomics analysis of serum of Holstein Friesian cows (confident (q-value < 0.01), likely (q-value < 0.05) and putative (q-value > 0.05 but p-value < 1-π0) proteins). Supplementary Figure 4. Volcano plots displaying the differentially abundant (DA) proteins identified by TMT-6plex quantitative proteomics analysis of serum of Holstein Friesian cows (confident (q-value < 0.01), likely (q-value < 0.05) and putative (q-value > 0.05 but p-value < 1-π0) proteins) (PDF)

■ AUTHOR INFORMATION

Corresponding Author

Rosa Casais − *Center for Animal Biotechnology, Servicio Regional de Investigación y Desarrollo Agroalimentario [SERIDA], 33394 Deva, Asturias, Spain;* orcid.org/0000-0001-8349-5878; Phone: 00 34 984502010; Email: rosacg@serida.org

Authors

Alejandra Isabel Navarro León − *Center for Animal Biotechnology, Servicio Regional de Investigación y Desarrollo Agroalimentario [SERIDA], 33394 Deva, Asturias, Spain*

Marta Muñoz − *Center for Animal Biotechnology, Servicio Regional de Investigación y Desarrollo Agroalimentario [SERIDA], 33394 Deva, Asturias, Spain*

Natalia Iglesias − *Center for Animal Biotechnology, Servicio Regional de Investigación y Desarrollo Agroalimentario [SERIDA], 33394 Deva, Asturias, Spain*

Cristina Blanco-Vázquez − *Center for Animal Biotechnology, Servicio Regional de Investigación y Desarrollo Agroalimentario [SERIDA], 33394 Deva, Asturias, Spain*

Ana Balseiro − *Departamento de Sanidad Animal, Facultad de Veterinaria, Universidad de León, 24071 León, Spain*

Fátima Milhano Santos − *Functional Proteomics Laboratory, National Center for Biotechnology, 28049 Madrid, Spain;* orcid.org/0000-0002-4041-1504

Sergio Ciordia − *Functional Proteomics Laboratory, National Center for Biotechnology, 28049 Madrid, Spain*

Fernando J. Corrales − *Functional Proteomics Laboratory, National Center for Biotechnology, 28049 Madrid, Spain;* orcid.org/0000-0002-0231-5159

Tania Iglesias − *Unidad de Consultoría Estadística, Servicios Científico-técnicos, Universidad de Oviedo, 33203 Gijón, Asturias, Spain*

Complete contact information is available at: https://pubs.acs.org/10.1021/acs.jproteome.3c00244

Author Contributions

#A.I.N.L. and M.M. have equally contributed to this study.

Notes

The authors declare no competing financial interest.

■ ACKNOWLEDGMENTS

This Project I+D+i project (PID2021-122197OR-C22) was funded by the MCIN/AEI/10.13039/501100011033/FEDER, UE and regional funds PCTI 2021−2023 (GRUPIN: IDI2021-000102). We acknowledge the National Institute for Agricultural Research (INIA) for the scholarships of Cristina Blanco Vázquez (CPD2016.0142 funded by MCIN/AEI/10.13039/50110001033 and FSE) and Alejandra Isabel Navarro (PRE20200-096451). We would like to acknowledge ASTEGA Veterinary Services for their collaboration in the sampling work and the daily work of SERIDA's farm operators in the care and maintenance of animals. We gratefully acknowledge Kevin P. Dalton for proofreading the manuscript.

■ REFERENCES

(1) Benedictus, G.; Dijkhuizen, A. A.; Stelwagen, J. Economic losses due to paratuberculosis in dairy cattle. *Vet Rec* **1987**, *121* (7), 142−146.
(2) Kudahl, A. B.; Nielsen, S. S.; Sørensen, J. T. Relationship between antibodies against Mycobacterium avium subsp. paratuberculosis in milk and shape of lactation curves. Pre. *Vet. Med.* **2004**, *62* (2), 119−134.
(3) Ozsvari, L.; Harnos, A.; Lang, Z.; Monostori, A.; Strain, S.; Fodor, I. The Impact of Paratuberculosis on Milk Production, Fertility, and Culling in Large Commercial Hungarian Dairy Herds. *Front. Vet. Sci.* **2020**, *7*, 565324.
(4) Smith, R. L.; Strawderman, R. L.; Schukken, Y. H.; Wells, S. J.; Pradhan, A. K.; Espejo, L. A.; et al. Effect of Johne's disease status on reproduction and culling in dairy cattle. *J. Dairy Sci.* **2010**, *93*, 3513−24.
(5) Tiwari, A.; VanLeeuwen, J. A.; Dohoo, I. R.; Stryhn, H.; Keefe, G. P.; Haddad, J. P. Effects of seropositivity for bovine leukemia virus, bovine viral diarrhoea virus, *Mycobacterium avium* subspecies *paratuberculosis*, and *Neospora caninum* on culling in dairy cattle in four Canadian provinces. *Vet. Microbiol.* **2005**, *109* (3−4), 147−58.

(6) Millar, D.; Ford, J.; Sanderson, J.; Withey, S.; Tizard, M.; Doran, T.; et al. IS900 PCR to detect *Mycobacterium paratuberculosis* in retail supplies of whole pasteurized cows' milk in England and Wales. *Appl. Environ. Microbiol.* **1996**, *62* (9), 3446−52.
(7) Grant, I. R.; Ball, H. J.; Neill, S. D.; Rowe, M. T. Inactivation of *Mycobacterium paratuberculosis* in Cows' Milk at Pasteurization Temperatures. *Appl. Environ. .Microbiol.* **1996**, *62* (2), 631−6.
(8) Monif, G. R. G. Translation of Hypothesis to Therapy in Crohn's Disease. *Inflamm. Bowel Dis.* **2016**, *22* (2), E8−9.
(9) Feller, M.; Huwiler, K.; Stephan, R.; Altpeter, E.; Shang, A.; Furrer, H.; et al. *Mycobacterium avium* subespecies *paratuberculosis* and Crohn's disease: a systematic review and meta-analysis. *Lancet Infect. Dis.* **2007**, *7* (9), 607−613.
(10) Kuenstner, J. T.; Naser, S.; Chamberlin, W.; Borody, T.; Graham, D. Y.; McNees, A.; et al. The consensus from the *Mycobacterium avium* ssp. *paratuberculosis* (MAP) Conference 2017. *Front. Public Health* **2017**, *5*, 208.
(11) Niegowska, M.; Rapini, N.; Piccinini, S.; Mameli, G.; Caggiu, E.; Manca Bitti, M. L.; Sechi, L. A.; et al. Type 1 diabetes at-risk children highly recognize *Mycobacterium avium* subspecies *paratuberculosis* epitopes homologous to human Znt8 and proinsulin. *Sci. Rep.* **2016**, *6*, 22266.
(12) Yokoyama, K.; Cossu, D.; Hoshino, Y.; Tomizawa, Y.; Momotani, E.; Hattori, N. Anti-mycobacterial antibodies in paired cerebrospinal fluid and serum samples from Japanese patients with multiple sclerosis or neuromyelitis optica spectrum disorder. *J. Clin. Med.* **2018**, *7* (12), 522.
(13) Mameli, G.; Cocco, E.; Frau, J.; Marrosu, M. G.; Sechi, L. A. Epstein-Barr virus and *Mycobacterium avium* subsp. *paratuberculosis* peptides are recognized in sera and cerebrospinal fluid of MS patients. *Sci. Rep.* **2016**, *6*, 22401.
(14) Bo, M.; Erre, G. L.; Niegowska, M.; Piras, M.; Taras, L.; Longu, M. G.; et al. Interferon regulatory factor 5 is a potential target of autoimmune response triggered by Epstein-Barr virus and *Mycobacterium avium* subsp. *paratuberculosis* in rheumatoid arthritis: investigating a mechanism of molecular mimicry. *Clin. Exp. Rheumatol.* **2018**, *36* (3), 376−381.
(15) Bo, M.; Niegowska, M.; Erre, G. L.; Piras, M.; Longu, M. G.; Manchia, P.; et al. Rheumatoid arthritis patient antibodies highly recognize IL-2 in the immune response pathway involving IRF5 and EBV antigens. *Sci. Rep.* **2018**, *8* (1), 1789.
(16) Sweeney, R. W. Pathogenesis of paratuberculosis. *Vet. Clin. North Am. Food Anim. Pract.* **2011**, *27* (3), 537−46.
(17) Whittington, R. J.; Sergeant, E. S. Progress towards understanding the spread, detection and control of *Mycobacterium avium* subsp. *paratuberculosis* in animal populations. *Aust. Vet. J.* **2001**, *79* (4), 267−278.
(18) Kudahl, A. B.; Nielsen, S. S.; Ostergaard, S. Strategies for time of culling in control of paratuberculosis in dairy herds. *J. Dairy Sci.* **2011**, *94* (8), 3824−34.
(19) Whitlock, R. H.; Wells, S. J.; Sweeney, R. W.; Van Tiem, J. ELISA and fecal culture for paratuberculosis (Johnés disease): sensitivity and specificity of each method. *Vet. Microbiol.* **2000**, *77* (3−4), 387−398.
(20) Mckenna, S. L. B.; Keefe, G. P.; Barkema, H. W.; Sockett, D. C. Evaluation of three ELISAs for *Mycobacterium avium* subsp. *paratuberculosis* using tissue and fecal culture as comparison standards. *Vet. Microbiol.* **2005**, *110* (1−2), 105−111.
(21) Nielsen, S. S.; Toft, N. Age-specific characteristics of ELISA and fecal culture for purpose-specific testing for paratuberculosis. *J. Dairy Sci.* **2006**, *89* (2), 569−579.
(22) Nielsen, S. S.; Toft, N. Ante mortem diagnosis of paratuberculosis: a review of accuracies of ELISA, interferon-γ assay and faecal culture techniques. *Vet. Microbiol.* **2008**, *129* (3−4), 217−235.
(23) Wells, S. J.; Collins, M. T.; Faaberg, K. S.; Wees, C.; Tavornpanich, S.; Petrini, K. R.; Collins, J. E.; Cernicchiaro, N.; Whitlock, R. H. Evaluation of a rapid fecal PCR test for detection of *Mycobacterium avium* subsp. *paratuberculosis* in dairy cattle. *Clin. Vaccine Immunol.* **2006**, *13* (10), 1125−1130.
(24) Seth, M.; Lamont, E. A.; Janagama, H. K.; Widdel, A.; Vulchanova, L.; Stabel, J. R.; Waters, W. R.; Palmer, M. V.; Sreevatsan, S. Biomarker discovery in subclinical mycobacterial infections of cattle. *PLoS One* **2009**, *4* (5), No. e5478.
(25) You, Q.; Verschoor, C. P.; Pant, S. D.; Macri, J.; Kirby, G. M.; Karrow, N. A. Proteomic analysis of plasma from Holstein cows testing positive for *Mycobacterium avium* subsp. *paratuberculosis* (MAP). *Vet. Immunol. Immunopathol.* **2012**, *148* (3−4), 243−251.
(26) Cha, S. B.; Yoo, A.; Park, H. T.; Sung, K. Y.; Shin, M. K.; Yoo, H. S. Analysis of transcriptional profiles to discover biomarker candidates in *Mycobacterium avium* subsp. *paratuberculosis*-infected macrophages, RAW 264.7. *J.Microbiol. Biotechnol.* **2013**, *23* (8), 1167−1175.
(27) David, J.; Barkema, H. W.; Guan, L. L.; De Buck, J. Gene-expression profiling of calves 6 and 9 months after inoculation with *Mycobacterium avium* subsp. *paratuberculosis*. *Vet. Res.* **2014**, *45* (1), 96.
(28) Shin, M. K.; Park, H.; Shin, S. W.; Jung, M.; Lee, S. H.; Kim, D. Y.; Yoo, H. S. Host transcriptional profiles and immunopathologic response following *Mycobacterium avium* subsp. *paratuberculosis* infection in mice. *PloS One* **2015**, *10* (10), No. e0138770.
(29) Shin, M. K.; Park, H. T.; Shin, S. W.; Jung, M.; Im, Y. B.; Park, H. E.; Cho, Y. I.; Yoo, H. S. Whole-blood gene-expression profiles of cows infected with *Mycobacterium avium* subsp. *paratuberculosis* reveal changes in immune response and lipid metabolism. *J. Microbiol. Biotechnol.* **2015**, *25* (2), 255−267.
(30) Hempel, R. J.; Bannantine, J. P.; Stabel, J. R. Transcriptional profiling of ileocecal valve of Holstein dairy cows infected with *Mycobacterium avium* subsp. *paratuberculosis*. *PLoS One* **2016**, *11* (4), No. e0153932.
(31) Malvisi, M.; Palazzo, F.; Morandi, N.; Lazzari, B.; Williams, J. L.; Pagnacco, G.; Minozzi, G. Responses of bovine innate immunity to *Mycobacterium avium* subsp. *paratuberculosis* infection revealed by changes in gene expression and levels of microRNA. *PLoS One* **2016**, *11* (10), No. e0164461.
(32) Berry, A.; Wu, C.; Venturino, A. J.; Talaat, A. M. Diomarkers for early stages of Johneś disease infection and immunization in goats. *Front. Microbiol.* **2018**, *9*, 2284.
(33) Van den Esker, M. H.; Koets, A. P. Application of transcriptomics to enhance early diagnostics of mycobacterial infections, with an emphasis on Mycobacterium avium sp. paratuberculosis. *Vet. Sci.* **2019**, *6* (3), 59.
(34) Palacios, A.; Sampedro, L.; Sevilla, I. A.; Molina, E.; Gil, D.; Azkargorta, M.; Elortza, F.; Garrido, J. M.; Anguita, J.; Prados-Rosales, R. *Mycobacterium tuberculosis* extracelular vesicle-associated lipoprotein LpqH as a potential biomarker to distinguish paratuberculosis infection or vaccination from tuberculosis infection. *BMC Vet. Res.* **2019**, *15* (1), 188.
(35) Purdie, A. C.; Plain, K. M.; Begg, D. J.; de silva, K.; Whittington, R. J. Gene expression profiles during subclinical mycobacterium avium subspecies paratuberculosis infection in sheep can predict disease outcome. *Sci. Rep.* **2019**, *9*, 8245.
(36) Shaughnessy, R. G.; Farrell, D.; Stojkovic, B.; Browne, J. A.; Kenny, K.; Gordon, S. V. Identification of microRNAs in bovine faeces and their potential as biomarkers of Johne's Disease. *Sci. Rep* **2020**, *10*, 5908.
(37) Alonso-Hearn, M.; Canive, M.; Blanco-Vazquez, C.; Torremocha, R.; Balseiro, A.; Amado, J.; Varela-Martinez, E.; Ramos, R.; Jugo, B. M.; Casais, R. RNA-Seq analysis of ileocecal valve and peripheral blood from Holstein cattle infected with Mycobacterium avium subsp, paratuberculosis revealed dysregulation of the CXCL8/IL8 signaling pathway. *Sci. Rep.* **2019**, *9*, 14845.
(38) Park, H. E.; Park, H. T.; Jung, Y. H.; Yoo, H. S. Establishment a real-time reverse transcription PCR based on host biomarkers for the detection of the subclinical cases of against *Mycobacterium avium* subsp. *paratuberculosis*. *PLoS One* **2017**, *12*, No. e0178336.
(39) Park, H. E.; Park, J. S.; Park, H. T.; Choi, J. G.; Shin, J. I.; Jung, M.; Kang, H. L.; Baik, S. C.; Lee, W. K.; Kim, D.; Yoo, H. S.; Shin, M. K. Alpha-2-Macroglobulin as a New Promising Biomarker Improving the Diagnostic Sensitivity of Bovine Paratuberculosis. *Front. Vet. Sci.* **2021**, *8*, 637716.

https://doi.org/10.1021/acs.jproteome.3c00244
J. Proteome Res. 2024, 23, 2762−2779

(40) Blanco-Vázquez, C.; Alonso-Hearn, M.; Juste, R. A.; Canive, M.; Iglesias, T.; Iglesias, N.; Amado, J.; Vicente, F.; Balseiro, A.; Casais, R. Detection of latent forms of *Mycobacterium avium* subsp. *paratuberculosis* infection using host biomarker-based ELISAs greatly improves paratuberculosis diagnostic sensitivity. *PLoS One* **2020**, *15* (9), No. e0236336.
(41) Blanco-Vázquez, C.; Balseiro, A.; Alonso-Hearn, M.; Juste, R. A.; Iglesias, N.; Canive, M.; Casais, R. Bovine Intelectin 2 expression as a biomarker of paratuberculosis disease progression. *Animals (Basel)* **2021**, *11* (5), 1370.
(42) Blanco-Vázquez, C.; Alonso-Hearn, M.; Iglesias, N.; Vázquez, P.; Juste, R. A.; Garrido, J. M.; Balseiro, A.; Canive, M.; Amado, J.; Queipo, M. A.; Iglesias, T.; Casais, R. Use of ATP-Binding Cassette Subfamly A Member 13 (ABCA13) for sensitive detection of focal pathological forms of subclinical bovine paratuberculosis. *Front. Vet. Sci.* **2022**, *9*, 816135.
(43) Wright, K.; Plain, K.; Purdie, A.; Saunders, B. M.; de Silva, K. Biomarkers for detecting resilience against Mycobacterial disease in animals. *Infect. Immun.* **2019**, *88* (1), No. e00401-19.
(44) Lamont, E. A.; Janagama, H. K.; Ribeiro-Lima, J.; Vulchanova, L.; Seth, M.; Yang, M.; Kurmi, K.; Waters, W. R.; Thacker, T.; Sreevatsan, S. Circulating Mycobacterium bovis peptides and host response proteins as biomarkers for unambiguous detection of subclinical infection. *J. Clin. Microbiol.* **2014**, *52* (2), 536−43.
(45) Sun, H.; Pan, L.; Jia, H.; Zhang, Z.; Gao, M.; Huang, M.; Wang, J.; Sun, Q.; Wei, R.; Du, B.; Xing, A.; Zhang, Z. Label-Free Quantitative Proteomics Identifies Novel Plasma Biomarkers for Distinguishing Pulmonary Tuberculosis and Latent Infection. *Front. Microbiol.* **2018**, *9*, 1267.
(46) Zhong, L.; Taylor, D.; Begg, D. J.; Whittington, R. J. Biomarker discovery for ovine paratuberculosis (Johnés disease) by proteomic serum profiling. *Comp. Immunol. Microbiol. Infect. Dis.* **2011**, *34* (4), 315−26.
(47) Phillips, I. L.; Danelishvili, L.; Bermudez, L. E. Macrophage proteome analysis at different stages of *Mycobacterium avium* subsp. *paratuberculosis* infection reveals a mechanism of pathogen dissemination. *Proteomes* **2021**, *9* (2), 20.
(48) Kleinwort, K. J. H.; Hobmaier, B. F.; Mayer, R.; Holzel, C.; Degroote, R. L.; Martlbauer, E.; Hauck, S. M.; Deeg, C. A. *Mycobacterium avium* subsp. *paratuberculosis* proteome changes profoundly in milk. *Metabolites* **2021**, *11*, 549.
(49) González, J.; Geijo, M. V.; García-Pariente, C.; Verna, A.; Corpa, J. M.; Reyes, L. E.; et al. Histopathological classification of lesions associated with natural paratuberculosis infection in cattle. *J. Comp. Pathol.* **2005**, *133*, 184−96.
(50) Ramos-Fernández, A.; Paradela, A.; Navajas, R.; Albar, J. P. Generalized method for probability-based peptide and protein identification from tandem mass spectrometry data and sequence database searching. *Mol. Cell Proteomics.* **2008**, *7* (9), 1748−54.
(51) Lopez-Serra, P.; Marcilla, M.; Villanueva, A.; Ramos-Fernandez, A.; Palau, A.; Leal, L.; Wahi, J. E.; Setien-Baranda, F.; Szczesna, K.; Moutinho, C.; Martinez-Cardus, A.; Heyn, H.; Sandoval, J.; Puertas, S.; Vidal, A.; Sanjuan, X.; Martinez-Balibrea, E.; Vinals, F.; Perales, J. C.; Bramsem, J. B.; Ørntoft, T. F.; Andersen, C. L.; Tabernero, J.; McDermott, U.; Boxer, M. B.; Heiden, M. G. V.; Albar, J. P.; Esteller, M. A DERL3-associated defect in the degradation of SLC2A1 mediates the Warburg effect. *Nat. Commun.* **2014**, *5*, 3608.
(52) *R: A Language and Environment for Statistical Computing*; R Foundation for Statisitical Computing: Vienna, Austria, 2021, https://www.r-project.org/.
(53) Muller, M. P.; Tomlinson, G.; Marrie, T. J.; Tang, P.; McGeer, A.; Low, D. E.; et al. Can routine laboratory tests discriminate between severe acute respiratory syndrome and other causes of community-acquired pneumonia? *Clin. Infect. Dis.* **2005**, *40*, 1079−10.
(54) Khovidhunkit, W.; Memon, R. A.; Feingold, K. R.; Grunfeld, C. Infection and inflammation-induced proatherogenic changes of lipoproteins. *J. Infect. Dis.* **2000**, *181* (Suppl 3), S462−72.
(55) Schultz, J. R.; Tu, H.; Luk, A.; Repa, J. J.; Medina, J. C.; Li, L.; Schwendner, S.; Wang, S.; Thoolen, M.; Mangelsdorf, D. J.; Lustig, K. D.; Shan, B. Role of LXRs in control of lipogenesis. *Genes Dev.* **2000**, *14* (22), 2831−8.
(56) Venkateswaran, A.; Laffitte, B. A.; Joseph, S. B.; Mak, P. A.; Wilpitz, D. C.; Edwards, P. A.; Tontonoz, P. Control of cellular cholesterol efflux by the nuclear oxysterol receptor LXR alpha. *Proc. Natl. Acad. Sci. U. S. A.* **2000**, *97* (22), 12097−102.
(57) Chiang, J. Y.; Kimmel, R.; Weinberger, C.; Stroup, D. Farnesoid X receptor responds to bile acids and represses cholesterol 7alpha-hydroxylase gene (CYP7A1) transcription. *J. Biol. Chem.* **2000**, *275* (15), 10918−24.
(58) Stayrook, K. R.; Bramlett, K. S.; Savkur, R. S.; Ficorilli, J.; Cook, T.; Christe, M. E.; Michael, L. F.; Burris, T. P. Regulation of carbohydrate metabolism by the farnesoid X receptor. *Endocrinology* **2005**, *146* (3), 984−91.
(59) Shaik, F. B.; Prasad, D. V.; Narala, V. R. Role of farnesoid X receptor in inflammation and resolution. *Inflamm Res.* **2015**, *64* (1), 9−20.
(60) Porez, G.; Gross, B.; Prawitt, J.; Gheeraert, C.; Berrabah, W.; Alexandre, J.; Staels, B.; Lefebvre, P. The hepatic orosomucoid/α1-acid glycoprotein gene cluster is regulated by the nuclear bile acid receptor FXR. *Endocrinology* **2013**, *154* (10), 3690−701.
(61) Gabay, C.; Kushner, I. Acute-phase proteins and other systemic responses to inflammation. *N. Engl. J. Med.* **1999**, *340* (6), 448−54.
(62) Hardardóttir, I.; Grünfeld, C.; Feingold, K. R. Effects of endotoxin and cytokines on lipid metabolism. *Curr. Opin. Lipidol.* **1994**, *5* (3), 207−15.
(63) Eckersall, P. D.; Bell, R. Acute phase proteins: Biomarkers of infection and inflammation in veterinary medicine. *Vet. J.* **2010**, *185* (1), 23−7.
(64) Zweigner, J.; Schumann, R. R.; Weber, J. R. The role of lipopolysaccharide-binding protein in modulating the innate immune response. *Microbes Infect* **2006**, *8* (3), 946−52.
(65) Vignal, C.; Guerardel, Y.; Kremer, L.; Masson, M.; Legrand, D.; Mazurier, J.; Elass, E. Lipomannans, but not lipoarabinomannans, purified from Mycobacterium chelonae and Mycobacterium kansasii induce TNF-alpha and IL-8 secretion by a CD14-toll-like receptor 2-dependent mechanism. *J. Immunol.* **2003**, *171* (4), 2014−23.
(66) Huang, X.; Zeng, Y.; Jiang, Y.; Qin, Y.; Luo, W.; Xiang, S.; Sooranna, S. R.; Pinhu, L. Lipopolysaccharide-Binding Protein Downregulates Fractalkine through Activation of p38 MAPK and NF-κB. *Mediators Inflamm* **2017**, *2017*, 9734837.
(67) Haapasalo, K.; van Kessel, K.; Nissilä, E.; Metso, J.; Johansson, T.; Miettinen, S.; Varjosalo, M.; Kirveskari, J.; Kuusela, P.; Chroni, A.; Jauhiainen, M.; van Strijp, J.; Jokiranta, T. S. Complement Factor H Binds to Human Serum Apolipoprotein E and Mediates Complement Regulation on High Density Lipoprotein Particles. *J. Biol. Chem.* **2015**, *290* (48), 28977−87.
(68) Ferreira, V. P.; Pangburn, M. K.; Cortés, C. Complement control protein factor H: the good, the bad, and the inadequate. *Mol. Immunol.* **2010**, *47* (13), 2187−97.
(69) Haapasalo, K.; Vuopio, J.; Syrjänen, J.; Suvilehto, J.; Massinen, S.; Karppelin, M.; Järvelä, I.; Meri, S.; Kere, J.; Jokiranta, T. S. Acquisition of complement factor H is important for pathogenesis of Streptococcus pyogenes infections: evidence from bacterial in vitro survival and human genetic association. *J. Immunol.* **2012**, *188*, 426−435.
(70) Ahmed, M. S.; Jadhav, A. B.; Hassan, A.; Meng, Q. H. Acute phase reactants as novel predictors of cardiovascular disease. *ISRN Inflamm* **2012**, *2012*, 953461.
(71) Turken, O.; Kunter, E.; Sezer, M.; Solmazgul, E.; Cerrahoglu, K.; Bozkanat, E.; Ozturk, A.; Ilvan, A. Hemostatic changes in active pulmonary tuberculosis. *Int. J. Tuberc. Lung Dis.* **2002**, *6* (10), 927−32.
(72) Li, M.; Wang, Z.; Zhu, L.; Shui, Y.; Zhang, S.; Guo, W. Down-regulation of RBP4 indicates a poor prognosis and correlates with immune cell infiltration in hepatocellular carcinoma. *Biosci. Rep.* **2021**, *41* (4), BSR20210328.
(73) Espinosa, J.; de la Morena, R.; Benavides, J.; García-Pariente, C.; Fernández, M.; Tesouro, M.; Arteche, N.; Vallejo, R.; Ferreras, M. C.; Pérez, V. Assessment of Acute-Phase Protein Response Associated with

the Different Pathological Forms of Bovine Paratuberculosis. *Animals (Basel)* **2020**, *10* (10), 1925.
(74) Stabel, J. R. Transitions in immune responses to Mycobacterium paratuberculosis. *Vet. Microbiol.* **2000**, *77*, 465−473.
(75) Fernandez, M.; Benavides, J.; Castano, P.; Elguezabal, N.; Fuertes, M.; Munoz, M.; Royo, M.; Ferreras, M. C.; Perez, V. Macrophage subsets within granulomatous intestinal lesions in bovine paratuberculosis. *Vet. Pathol.* **2017**, *54*, 82−934.
(76) Smeed, J. A.; Watkins, C. A.; Rhind, S. M.; Hopkins, J. Differenctial cytokine gene expression profiles in the three pathological forms of shhepp paratuberculosis. *BMC Vet. Res.* **2007**, *3*, 18.
(77) Staprans, I.; Felts, J. M. The effect of alpha1-acid glycoprotein (orosomucoid) on triglyceride metabolism in the nephrotic syndrome. *Biochem. Biophys. Res. Commun.* **1977**, *79* (4), 1272−8.
(78) Lee, Y. S.; Choi, J. W.; Hwang, I.; Lee, J. W.; Lee, J. H.; Kim, A. Y.; Huh, J. Y.; Koh, Y. J.; Koh, G. Y.; Son, H. J.; Masuzaki, H.; Hotta, K.; Alfadda, A. A.; Kim, J. B. Adipocytokine orosomucoid integrates inflammatory and metabolic signals to preserve energy homeostasis by resolving immoderate inflammation. *J. Biol. Chem.* **2010**, *285* (29), 22174−85.
(79) Hotta, K.; Funahashi, T.; Bodkin, N. L.; Ortmeyer, H. K.; Arita, Y.; Hansen, B. C.; Matsuzawa, Y. Circulating concentrations of the adipocyte protein adiponectin are decreased in parallel with reduced insulin sensitivity during the progression to type 2 diabetes in rhesus monkeys. *Diabetes* **2001**, *50* (5), 1126−33.
(80) Maeda, N.; Shimomura, I.; Kishida, K.; Nishizawa, H.; Matsuda, M.; Nagaretani, H.; Furuyama, N.; Kondo, H.; Takahashi, M.; Arita, Y.; Komuro, R.; Ouchi, N.; Kihara, S.; Tochino, Y.; Okutomi, K.; Horie, M.; Takeda, S.; Aoyama, T.; Funahashi, T.; Matsuzawa, Y. Diet-induced insulin resistance in mice lacking adiponectin/ACRP30. *Nat. Med.* **2002**, *8* (7), 731−7.
(81) Sparks, J. D.; Sparks, C. E. Insulin modulation of hepatic synthesis and secretion of apolipoprotein B by rat hepatocytes. *J. Biol. Chem.* **1990**, *265* (15), 8854−62.
(82) Jones, J. I.; Clemmons, D. R. Insulin-like growth factors and their binding proteins: biological actions. *Endocr. Rev.* **1995**, *16*, 3−34.
(83) Wheatcroft, S. B.; Kearney, M. T.; Shah, A. M.; Ezzat, V. A.; Miell, J. R.; Modo, M.; Williams, S. C.; Cawthorn, W. P.; Medina-Gomez, G.; Vidal-Puig, A.; Sethi, J. K.; Crossey, P. A. IGF-binding protein-2 protects against the development of obesity and insulin resistance. *Diabetes* **2007**, *56* (2), 285−94.
(84) Dong, J.; Yu, J.; Li, Z.; Gao, S.; Wang, H.; Yang, S.; Wu, L.; Lan, C.; Zhao, T.; Gao, C.; Liu, Z.; Wang, X.; Hao, J. Serum insulin-like growth factor binding protein 2 levels as biomarker for pancreatic ductal adenocarcinoma-associated malnutrition and muscle wasting. *J. Cachexia Sarcopenia Muscle* **2021**, *12* (3), 704−716.
(85) Yakovenko, A.; Cameron, M.; Trevino, J. G. Molecular therapeutic strategies targeting pancreatic cancer induced cachexia. *World J. Gastrointest. Surg.* **2018**, *10*, 95.
(86) Lescuyer, P.; Hochstrasser, D.; Rabilloud, T. How shall we use the proteomics toolbox for biomarker discovery? *J. Proteome Res.* **2007**, *6* (9), 3371−6.
(87) Eckersall, P. D.; Young, F. J.; McComb, C.; Hogarth, C. J.; Safi, S.; Weber, A.; McDonald, T.; Nolan, A. M.; Fitzpatrick, J. L. Acute phase proteins in serum and milk from dairy cows with clinical mastitis. *Vet Rec* **2001**, *148* (2), 35−41.
(88) Prohl, A.; Schroedl, W.; Rhode, H.; Reinhold, P. Acute phase proteins as local biomarkers of respiratory infection in calves. *BMC Vet Res.* **2015**, *11*, 167.
(89) Bagga, A.; Randhawa, S. S.; Sharma, S.; Bansal, B. K. Acute phase response in lame crossbred dairy cattle. *Vet World* **2016**, *9* (11), 1204−1208.
(90) Joshi, V.; Gupta, V. K.; Bhanuprakash, A. G.; Mandal, R. S. K.; Dimri, U.; Ajith, Y. Haptoglobin and serum amyloid A as putative biomarker candidates of naturally occurring bovine respiratory disease in dairy calves. *Microb Pathog* **2018**, *116*, 33−37.
(91) Hajek, F.; Reus, A.; Gruber, S.; Plattner, S.; Kammer, M.; Baumgartner, C.; Smink, M.; Döpfer, D.; Hachenberg, S.; Mansfeld, R. Nutzung der Haptoglobinkonzentration im Blutserum als Indikator im Tiergesundheitsmonitoring bei Milchkühen [Use of serum haptoglobin concentration as an indicator in animal health monitoring of dairy cows]. *Tierarztl Prax Ausg G Grosstiere Nutztiere* **2020**, *48* (4), 228−238.
(92) Raj, A.; Kulangara, V.; Vareed, T. P.; Melepat, D. P.; Chattothayil, L.; Chullipparambil, S. Variations in the levels of acute-phase proteins and lactoferrin in serum and milk during bovine subclinical mastitis. *J. Dairy Res.* **2021**, *88* (3), 321−325.

https://doi.org/10.1021/acs.jproteome.3c00244
J. Proteome Res. 2024, 23, 2762−2779